Calcium-dependent cytosolic phospholipase A2 activation is implicated in neuroinflammation and oxidative stress associated with ApoE4

Shaowei Wang
USC: University of Southern California
Boyang Li
University of Southern California
Victoria Solomon
University of Southern California
Alfred Fonteh
Huntington Medical Research Institutes
Stanley I. Rapoport
NIAAA: National Institute on Alcohol Abuse and Alcoholism
David A. Bennett
Rush University Medical Center
Zoe Arvanitakis
Rush University Medical Center
Helena C. Chui
USC: University of Southern California
Carol A. Miller
USC: University of Southern California
Patrick M. Sullivan
Duke University
Hoau-Yan Wang
CUNY: City University of New York
Hussein Yassine (hyassine@usc.edu)
University of Southern California https://orcid.org/0000-0002-2483-649X

Research article

Keywords: cPLA2, ApoE4, Alzheimer's disease, p38, Oxidative stress

Posted Date: January 20th, 2021

DOI: https://doi.org/10.21203/rs.3.rs-68804/v2

Version of Record: A version of this preprint was published at Molecular Neurodegeneration on April 16th, 2021. See the published version at https://doi.org/10.1186/s13024-021-00438-3.

Abstract

Background: Apolipoprotein E4 (*APOE4*) is associated with a greater response to neuroinflammation and the risk of developing late-onset Alzheimer's disease (AD), but the mechanisms for this association are not clear. The activation of calcium-dependent cytosolic phospholipase A2 (cPLA2) is involved in inflammatory signaling and is elevated within the plaques of AD brains. The relation between *APOE4* genotype and cPLA2 activity is not known.

Methods: Mouse primary astrocytes, mouse and human brain samples differing by *APOE* genotypes were collected for measuring cPLA2 expression, phosphorylation, and activity in relation to measures of inflammation and oxidative stress.

Results: Greater cPLA2 phosphorylation and activity was identified in ApoE4 compared to ApoE3 in primary astrocytes and brains of ApoE-targeted replacement (ApoE-TR) mice. These differences were also demonstrated in brain homogenates from the inferior frontal cortex from AD patients carrying *APOE3/4* compared to *APOE3/3*. Higher cPLA2 activation with *APOE4* was associated with greater activation of the MAPK p38 pathway in human postmortem frontal cortical synaptosomes and astrocytes, as well as with higher levels of leukotriene B4 (LTB4), reactive oxygen species (ROS), and inducible nitric oxide synthase (iNOS) in astrocytes. Inhibition of cPLA2 reduced LTB4, ROS, and iNOS levels in ApoE4 primary astrocytes to those in ApoE3 astrocytes.

Conclusions: Our findings implicate greater activation of cPLA2 signaling system with *APOE4*, which could represent a potential drug target for mitigating the increased neuroinflammation with *APOE4* and AD.

Background

The enzyme phospholipase A2 (PLA2) catalyzes the hydrolysis of the stereospecifically numbered (*sn*-2) ester bond of substrate phospholipids in the cell membrane to produce a free fatty acid and a lysophospholipid [1]. Calcium-independent PLA2 (iPLA2) has a greater affinity for releasing docosahexaenoic acid (DHA, 22:6 n-3), which acts as a signaling molecule during neurotransmission and as the precursor of anti-inflammatory and antioxidant resolvins [2, 3]. Calcium-dependent cytosolic phospholipase A2 (cPLA2) releases arachidonic acid (AA, 20:4 n-6), which plays important functions in storing energy, as a second messenger in neurotransmission, and as the precursor of eicosanoids [4, 5]. Free AA can be oxidized by cyclooxygenase (COX) or lipoxygenase (LOX) to produce prostaglandins or leukotrienes, which are potent mediators of inflammation [1, 6]. In astrocytes, cPLA2 interacts with mitochondrial antiviral-signaling protein (MAVS) to boost nuclear factor kappa-light-chain-enhancer of activated B cell (NF-kB)-driven inflammatory responses [7]. In microglia, cPLA2 and AA metabolic pathways contribute to reactive oxygen species (ROS) and nitric oxide (NO) production during cell activation[8]. cPLA2 activity depends on its phosphorylation, regulated by mitogen-activated protein kinase (MAPK) pathways [9, 10].

A lower amount of Ab oligomers and the absence of glial activation markers in both astrocytes and microglia distinguish the brains of individuals with greater brain Ab plaques and tangles but resilience to AD dementia from those with dementia [11]. cPLA2 activation is one of the pathways that activates microglia and astrocytes in the brain. The cPLA2 gene, protein levels, and phosphorylated form are increased around AD brains' plaques compared to healthy controls [12-14]. Increased activation of cPLA2 is observed in the hippocampus of human amyloid precursor protein (hAPP) transgenic mice [14]. The activation of cPLA2 by Ab oligomers contributes to dysregulation of fatty acid metabolism and promotes neurodegeneration [15, 16]. Overexpression of p25 (Protein 25, a cyclin-dependent kinase 5 activator) in neurons increases the expression of cPLA2, leading to lysophosphatidylcholine (LPC) secretion and the activation of astrocytes and production of proinflammatory cytokines [17]. Conversely, cPLA2 deficiency in AD mouse models ameliorates the memory impairment and hyperactivated glial cells observed in AD mouse models [14, 18]. Knocking out cPLA2 in microglia decreases lipopolysaccharide (LPS) induced oxidative stress and inflammatory response [8].

Carrying the *APOE4* allele is the strongest genetic risk factor for late-onset AD. The ApoE4 protein seems to have proinflammatory and/or reduced anti-inflammatory functions, which could exacerbate AD pathology. This ApoE4 effect on inflammation was clearly demonstrated in the Framingham cohort, where participants with *APOE4* and elevated plasma C-reactive protein (CRP) levels had a greater risk of developing late-onset of AD than age and sex-matched *APOE2* and *APOE3* carriers [19]. In the brains of participants with AD, *APOE4* is associated with greater levels of lipid peroxidation, eicosanoids, and oxidative stresses markers [20], but the mechanisms for these observations are not clear. Here, we hypothesized that ApoE4 activates cPLA2 to enhance AA release and eicosanoid levels, leading to an enhanced inflammatory and oxidative stress response. Accordingly, we examined cPLA2 expression and activation in mouse primary astrocytes, and in mouse, and human brain samples that differed by *APOE* genotype and determined the cellular effects of cPLA2 inhibition on measurements of neuroinflammation and oxidative stress.

Results

1. cPLA2 and phosphorylated cPLA2 are increased in ApoE4 mouse primary astrocytes

We previously found that DHA/AA ratio in cerebrospinal fluid (CSF) is lower in *APOE4/E4* carriers compared to *APOE3/E3* carriers [21, 22]. Since astrocytic cPLA2 and iPLA2 enzymes are important determinants of brain AA and DHA metabolism [2, 23], these enzymes' expression and activity were first examined in primary astrocytes from ApoE-TR mice. ApoE4 astrocytes had greater mRNA and protein levels of cPLA2 and phosphorylated cPLA2 compared with ApoE3 astrocytes (Fig. 1A, B). In contrast, iPLA2 mRNA and protein levels did not differ between ApoE4 and ApoE3 primary astrocytes (Fig.1C, D). These measures were also significantly greater in ApoE4 immortalized astrocytes compared to ApoE3 (Fig. S1). To identify cellular cPLA2 localization, cytosolic and membrane fractions were obtained from primary ApoE astrocytes. As expected, the majority of cPLA2 was present in the cytosol. Both cytosolic and membrane-bound cPLA2 levels were greater in ApoE4 compared to ApoE3 (Fig. S2). To further

explore the activities of cPLA2 and iPLA2, the efflux of ^{3}H-AA or ^{14}C-DHA from ApoE3 and ApoE4 primary astrocyte cells to media with or without ATP stimulation for 15 min was examined. ^{3}H-AA efflux was significantly greater in stimulated ApoE4 compared to ApoE3 primary astrocytes (Fig. 1E), whereas ^{14}C-DHA efflux showed no difference between ApoE4 and ApoE3 (Fig. 1F). To confirm the ApoE protein's effect, cultured primary astrocytes from C57BL/6 mice were labeled with ^{3}H-AA or ^{14}C-DHA and then treated with 0.2 μM rApoE3 or rApoE4 proteins for 24h under similar conditions to primary astrocytes cultured from ApoE-TR mice. ^{3}H-AA efflux was greater after rApoE4 than rApoE3 treatment (Fig. 1G), whereas DHA efflux did not differ between rApoE4 and rApoE3 treatments (Fig. 1H). Taken together, these results confirmed that cPLA2 expression and activity were greater in ApoE4 compared to ApoE3 astrocytes.

2. Phosphorylated cPLA2 and cPLA2 activity are increased in *APOE4* mouse brains

To investigate the effect of the ApoE isoforms on cPLA2 *in vivo*, mRNA, total protein, and phosphorylated protein levels of cPLA2 were measured in the cerebral cortex from 8-month-old ApoE3-TR and ApoE4-TR mice. There was no difference in cortical cPLA2 mRNA levels between ApoE3-TR and ApoE4-TR mice (Fig. 2A). Since phosphorylated cPLA2 levels were too low to detect in total brain homogenates, cPLA2 was enriched by immunoprecipitation with a cPLA2 antibody using 500 μg of cortical homogenate, and total and phosphorylated cPLA2 levels were measured by Western blot. Total cPLA2 levels did not differ between ApoE3-TR and ApoE4-TR mouse cortex (Fig. 2B, C). However, phosphorylated cPLA2 was significantly increased in the ApoE4-TR mouse cortex compared to the ApoE3-TR mouse cortex (Fig. 2B, C). Consistent with these observations, cortical cPLA2 activity (based on the hydrolysis of the arachidonoyl thioester bond to release a detectable free thiol by endogenous brain PLA2) and leukotriene B4 (LTB4) levels (downstream product of AA release after cPLA2 activation) were higher in ApoE4-TR than ApoE3-TR mice (Fig. 2D, E).

3. p38 MAPK but not ERK1/2 is increased in ApoE4 mouse primary astrocytes

Phosphorylation of cPLA2 is regulated by MAPK pathways, including p38 MAPK and ERK1/2 MAPK [10, 24, 25]. We tested the phosphorylation of p38 and ERK1/2 in primary astrocytes and mouse cortex from ApoE3 or ApoE4-TR mice by immunoblot using antibodies against total and phosphorylated proteins. Total p38 and ERK1/2 proteins did not differ between ApoE3 and ApoE4 primary astrocytes (Fig. 3A). Interestingly, only phosphorylated p38, but not phosphorylated ERK1/2, was significantly greater in ApoE4 primary astrocytes than ApoE3 primary astrocytes (Fig. 3A). In agreement, greater p38 phosphorylation but not ERK1/2 was evident in the cerebral cortex of 8-months old ApoE4-TR mice compared to ApoE3-TR mice (Fig. 3B). To test whether cPLA2 activation is dependent on p38 MAPK signaling, we treated ApoE4 primary astrocytes with two different p38 MAPK pathway inhibitors (SB202190 and SB203580) prior to the induction of cPLA2 activation with TNFa and IFNγ. The results showed that SB202190 significantly reduced phosphorylated (activated) cPLA2 levels (Fig. 3C). Interestingly, SB203580 had no inhibitory effects on cPLA2 activation (Fig. 3C), as SB203580 inhibited MAPKAPK-2 activity but not phosphorylation of p38 MAPK itself [26]. cPLA2 was found to be complexed with p38 as indicated by p38

co-immunoprecipitating with cPLA2 by anti-cPLA2 antibodies in immortalized ApoE4 astrocytes (Fig. 3D). These observations confirmed that p38 MAPK but not the ERK1/2 MAPK pathway can directly regulate cPLA2 phosphorylation.

4. phosphorylated cPLA2 is increased in *APOE4* human brains

Table 1 Characteristics of clinical samples

Regions sampled and source	Inferior frontal lobe (ROSMAP, RUSH ADRC)				Hippocampus, USC ADRC	
Clinical diagnosis	AD	AD	NCI	NCI	NCI	AD
Genotype	E3/E3	E3/E4	E3/E3	E3/E4	E3/E3	E4/E4
Sample size, n	12	10	12	10	7	9
Age (years ± SD) *	92±6	95±5	83±5	85±4	85±5	78±6
Sex (n, female/male) *	5/7	6/4	6/6	5/5	5/2	6/3
Braak stage	IV	V	III	III	I	V

*Age and gender did not differ between groups compared using ANOVA. NCI=no cognitive impairment. AD=Alzheimer's disease.

To determine whether these findings can be demonstrated in human brains, we first compared the total and phosphorylated forms of cPLA2 in human hippocampus samples from individuals with no cognitive impairment (NCI) and homozygous *APOE3 (APOE3/E3)* carriers with individuals with AD and homozygous *APOE4 (APOE4/E4)*. Characteristics of brain samples tested are summarized in Table 1. After enrichment of cPLA2 protein, phosphorylated and total protein levels of cPLA2 were detected by Western Blot. There was no difference in total cPLA2 protein between *APOE3/E3* and *APOE4/E4* human hippocampus, while phosphorylated cPLA2 trended toward an increase in *APOE4/E4* human hippocampus compared to that of *APOE3/E3* carriers. However, this difference did not reach statistical significance, likely due to the small human brain sample size (Fig. 4A). Moreover, this comparison was limited by virtue of a comparison that included both disease state and *APOE* genotype. To overcome this limitation, we compared phosphorylated and total cPLA2 in the inferior frontal cortex of persons with a similar clinical diagnosis but with different *APOE* genotypes. After a similar enrichment of cPLA2 from the cortex, phosphorylated and total cPLA2 levels were measured by Western Blot. In the NCI group, total cPLA2 did not significantly differ between the *APOE3/E3* and *APOE3/E4* carriers, while the phosphorylated cPLA2 level showed a trend increase in *APOE3/E4* carriers compared to *APOE3/E3* carriers (Fig. 4B). In patients with AD, phosphorylated cPLA2 levels were significantly greater in *APOE3/*E4 carriers compared with *APOE3/E3* carriers ($p=0.039$), while the total cPLA2 levels did not differ between the two groups (Fig. 4C). Greater cPLA2 phosphorylation in the *APOE3/4* group was not affected by sex,

age, or Braak stage. A nonsignificant difference in soluble Ab42 monomers (p=0.12) was observed in the brains of *APOE3/*E4 carriers compared with *APOE3/E3* carriers with AD (Supplementary Fig 3).

5. p38 MAPK is increased in *APOE4* human brain samples

Previous results from mouse astrocyte and cortex showed increased p38 activation in ApoE4-TR compared to ApoE3-TR mice. In agreement, greater levels of phosphorylated p38 in the hippocampus of the *APOE4/E4* AD group were observed compared to the *APOE3/E3* NCI group (Fig. 5A). Phosphorylated and total p38 levels did not differ between NCI *APOE3/E3* and NCI *APOE3/E4* groups (Fig. 5B), while total p38 level was significantly greater in the AD *APOE3/E4* group compared with the AD *APOE3/E3* group (Fig. 5C). These results support that the greater activation of cPLA2 in ApoE4 might be regulated by the p38 MAPK pathway and is most prominent in persons with AD.

6. LTB4 levels are increased in *APOE4* human brain samples

AA is released by cPLA2 hydrolysis of membrane phospholipids, and then can be rapidly oxidized by COX or LOX enzymes to prostaglandins or leukotrienes (LTB4 and PGE2), potent mediators of inflammation and signal transduction [2]. To test the effect of the greater cPLA2 phosphorylation in *APOE4* AD brains, PGE2 and LTB4 levels were assayed in brain homogenates from the inferior frontal cortex. LTB4 levels were significantly greater in the AD *APOE3/4* group compared with the AD *APOE3/3* group (p=0.01) (Fig. 6A), while PGE2 levels did not differ between the two groups (Fig. 6B). The greater LTB4 levels in APOE3/E4 group were also not affected by sex, age, or Braak stage. No significant differences were found in either LTB4 or PGE2 levels between the NCI *APOE3/4* and NCI *APOE3/4* groups (Fig. 6C and D). The expression of 5-LOX and COX-2 did not differ between the AD *APOE3/3* and AD *APOE3/4* groups (Fig. 6E). These results indicate that ApoE4's activation of cPLA2 in AD selectively increases LTB4 levels in the AD brain.

7. The NF-kB inflammasome is not induced in the *APOE4* brain

It is not clear whether *APOE4* can induce neuroinflammation via activation of the NF-kB inflammasome *in vivo*, and whether cPLA2 is involved in this pathway. Although we found greater TNFa mRNA levels in ApoE4 than in ApoE3 astrocytes, IL1b, IL6 and Ccl2 did not differ between ApoE3 and ApoE4 astrocytes (Fig. 7A). In addition, the protein levels of these cytokines and chemokines were comparable in different ApoE genotypes in the mouse brains (Fig. 7B) or the human brain samples (Fig. 7D). Similarly, the abundance of glial fibrillary acid protein (GFAP) in astrocytes and ionized calcium binding adaptor molecule 1 (Iba1) in microglia also did not differ by genotype (Fig. 7D-E). These results indicate that neuroinflammation with *APOE4* does not favor the NF-kB inflammatory response pathway.

8. cPLA2 is involved in the ApoE4 mediated up-regulation of LTB4 and ROS

To explore whether cPLA2 inhibition mitigates the downstream effects of LTB4 production on ROS and iNOS, ApoE3 and ApoE4 primary astrocytes were treated with the cPLA2 inhibitor pyrrophenone (Fig 8A). Treatment with pyrrophenone reduced LTB4 levels in ApoE3 and ApoE4 astrocytes, but to a greater extent

in ApoE4 astrocytes (Fig. 8B). Furthermore, cPLA2 inhibition significantly decreased iNOS and ROS levels in ApoE3 and ApoE4 primary astrocytes (Fig. 8C, D). These results indicated that greater cPLA2 activity promoted greater levels of iNOS and ROS in the ApoE4 group and can be reduced with cPLA2 inhibition. To confirm the specific effect of cPLA2 in LTB4 production, we knocked down cPLA2 by small interfering RNA (siRNA) in ApoE4 primary astrocytes (Fig. 8E). We found that LTB4 levels were significantly decreased in the cPLA2 siRNA treatment group compared to the non-target siRNA treatment group (Fig. 8F).

9. ApoE4 and Ab induce cPLA2 activation in human postmortem frontal cortical synaptosomes

Since cPLA2 was shown to be expressed in neurons and activated by Ab monomers[27], we examined the effect of exogenous Ab_{42} and ApoE on its activation in synaptosomes from human postmortem frontal cortices obtained from control participants without AD pathology. The results showed that treatment with Ab_{42}, ApoE4, ApoE4/Ab_{42} or ApoE3 individually had no effect on cPLA2 activation and distribution in cytosol and membrane of the synaptosomes (Fig. 9A, B). However, pretreatment with Ab_{42}, ApoE4 and Ab_{42} plus ApoE4 significantly prevented TNFa+IFNγ-evoked cPLA2 cytosol to membrane translocation leading to an increase in phosphorated cPLA2/cPLA2 ratio in the membranous fraction of synaptosome but a decrease in the cytosolic phosphorylated cPLA2/cPLA2 ratio. ApoE3 had no effect on cPLA2 activation (Fig. 9A, C). In contrast to TNFa+IFNγ, ceramide-1-phosphate did not alter cPLA2 cellular distribution. Ab_{42}, ApoE4 and Ab_{42} plus ApoE4 significantly enhanced phosphorylated cPLA2 levels in the cytosolic but had no effect on the membranous cPLA2 (Fig. 9A, D). Taken together, these results indicated that ApoE4 and Ab_{42} could induce cPLA2 activation in neurons and astrocytes, suggesting that greater cPLA2 activitation in the human cortex of AD E3/E4 compared to AD E3/E3 might arise from the combined effects of ApoE4 and greater Ab_{42} accumulation.

Discussion

Despite multiple past observations associating *APOE4* with greater neuroinflammatory and oxidative stress response than *APOE2* or *APOE3* (Table 2), the underlying mechanisms are not clearly understood. Here, we identify a plausible mechanism where *APOE4* induces greater activation of the MAPK p38-cPLA2 system, leading to greater release of AA, LTB4, iNOS, and generation of ROS in astrocytes. ApoE4 and Ab42 induced greater activation of cPLA2 in post mortem frontal lobe synaptosomes. The increase in LTB4 in *APOE4* was corroborated in human brain samples matched by disease state. Inhibition of cPLA2 activity lowered the greater neuroinflammation associated with *APOE4*, reinforcing the candidacy of cPLA2 as a therapeutic target for mitigating the increase in AD risk conferred by carrying *APOE4*.

Table 2. Summary of the association of *APOE4* with greater neuroinflammation.

Author	Key findings
Cultures (microglia, astrocytes, or mixed cultures) and inflammatory response by genotype	
Vitek et al. [28]	Microglia derived from ApoE4-TR mice demonstrate increased NO production, increased NOS2 mRNA levels, and greater TNFα, IL-6, IL12 levels compared to microglia from ApoE3-TR mice.
Colton et al. [29]	Significantly more NO was produced in primary microglia and macrophages from ApoE4-TR mice compared to ApoE3-TR mice.
Guo et al. [30]	The addition of exogenous ApoE4 induced greater IL1β than apoE3 in rat mixed glial cells.
Chen et al. [31]	ApoE4, but not ApoE3, stimulated secretion of PGE2 and IL-1β in rat primary microglia.
Shi et al. [32]	Higher TNFα, IL1β, and IL1α levels were observed in primary microglia from ApoE4-TR mice stimulated with LPS than ApoE2 and ApoE3.
Tai et al. [33]	Greater astrogliosis and microgliosis, higher levels of IL1β in E4FAD mice compared with E3FAD and E2FAD mice.
Zhu et al. [34]	Higher levels of microglia/macrophage, astrocytes, and invading T-cells after LPS injection in ApoE4-TR mice than ApoE3-TR mice. ApoE4-TR mice also displayed greater and more prolonged increases of cytokines (IL1β, IL6, TNFα) than ApoE2 and ApoE3-TR mice.
Ophir et al. [35]	The expression of inflammation-related genes (NF-κB response elements) following intracerebroventricular injection of LPS was significantly higher and more prolonged in ApoE4 than in ApoE3-TR mice.
Both human and mouse models	
Gale et al. [36]	ApoE4-TR mice displayed enhanced plasma cytokines after systemic LPS compared with ApoE3 counterparts. After intravenous LPS, *APOE3/4* patients had higher plasma TNF-α levels than *APOE3/3* patients.
Human brain studies of inflammation and oxidative stress studies by *APOE* genotype	
Montine at al [37]	Pyramidal neuron cytoplasm was immunoreactive for 4-hydroxy-2-nonenal (HNE) in 4 of 4 *APOE4* homozygotes, 2 of 3 *APOE3/4* heterozygotes, and none of 3 *APOE3* homozygotes
Ramassamy et al. [20]	In hippocampal homogenates from AD brains, *APOE4* carriers had greater levels of thiobarbituric acid-reactive substances (TBARS), lower catalase activities, and glutathione peroxidase and glutathione than tissues from patients homozygous for the *APOE3* allele (n=10 per group).
Egensperger et al. [38]	The number of activated microglia and the tissue area occupied by these cells increased

	significantly with the *APOE4* gene dose (n=20).
Minett et al. [39]	*APOE4* allele was significantly related to greater expression of CD68, HLA-DR, and CD64 in microglia (n=299).
Friedberg et al. [40]	Cellular density of microglial marker-Iba1 was positively associated with tau pathology in *APOE4* carrier participants only (n=154).
Systemic inflammation and dementia risk by genotype	
Tao et al. [19]	Participants with *APOE4* and elevated plasma C reactive protein (CRP) levels had a shortened latency for the onset of AD (n=2562).

There is evidence from clinical studies implicating greater cPLA2 activation around AD brain plaques [12]. cPLA2 activity is also increased in the CSF of patients with AD [41]. cPLA2 activation can be indirectly assessed by the release of AA from membrane phospholipids [2]. ^{11}C AA brain uptake by PET and unesterified AA/DHA measurement in CSF are surrogate brain cPLA2 activity markers. Indeed, greater incorporation coefficients of ^{11}C AA by PET scans were observed in the grey-matter regions of the brain of AD patients compared to control subjects [42]. Moreover, a greater AA/DHA ratio in both CSF and plasma was present in *APOE4* carriers with mild AD compared to *APOE3* carriers after DHA supplementation [21]. A greater AA/DHA ratio in plasma phospholipids in cognitively healthy *APOE4* carriers was associated with greater conversion to MCI/AD [43]. The greater plasma AA/DHA in *APOE4* suggests a systemic (for example, in the liver and adipose tissues) activation of cPLA2 that is not just confined to the brain.

Our studies in human brains revealed that carrying an *APOE4* allele is not sufficient to activate cPLA2. This is not surprising as not all *APOE4* carriers develop AD pathology. cPLA2 activation was significantly greater in *APOE4* carriers compared to *APOE3* carriers with AD, but not in those with NCI. One biological explanation is that the effects of soluble Ab oligomers in AD is additively intensified by ApoE4 to promote neuroinflammatory phenotype. We speculate that treatments which reduce activation of cPLA2 especially in *APOE4* carriers can protect these subjects from neuroinflammation and neurodegeneration, but this hypothesis is yet to be proven. In contrast to observations made in human brains, the activation of cPLA2 in APOE4 KI in both primary astrocytes and animal brain was measured independent of Ab. The APOE4 KI models used here are *APOE4* homozygous that maintained under a controlled environment to allow for observing a greater ApoE4 effect than studies with human brain samples.

Greater cPLA2 activation is mechanistically involved in AD pathology and may represent one pathophysiological link between Aβ oligomers and neuroinflammatory responses [44]. An increase of phosphorylated cPLA2 but not of total cPLA2 was observed in the brains of AD mouse models compared with WT mice [14]. In *vitro* studies suggested that Ab oligomers can trigger cPLA2 activation and PGE2 production in neurons, eventually leading to neurodegeneration [27, 45]. Inhibition of cPLA2 prevented synaptic loss and memory deficits induced by Ab oligomers in mice [46]. Similar to Ab, there is evidence

that human prion peptide can also induce neurotoxicity by activating cPLA2, which can be prevented by cPLA2 inhibition [47]. In support of greater cPLA2 activity, hippocampal levels of AA and AA-derived metabolites were much greater in hAPP mice than in non-transgenic control mice [48].

The pattern of enhanced neuroinflammation of the *APOE4* AD brains observed in this study does not support the induction of the NF-κB inflammasome by cytokines or chemokines such as TNFa, IL1b, IL6, and Ccl2, as past findings supporting these activation patterns were mostly a result of high doses LPS injections in cell culture and *in vivo* animal models (summarized in Table 2). Instead, we found a greater level of leukotrienes (LTB4) in the cerebral cortex of AD with E3/E4 carriers compared to E3/E3 carriers and ApoE4 astrocytes, which was associated with the greater phosphorylation of cPLA2. These observations provide a mechanism for the greater levels of oxidative stress in the *APOE4* brain [20, 37]. It is plausible that astrocytes and microglia contribute to the greater LTB4, ROS, and iNOS production with *APOE4*. An extensive recent proteomic and lipidomic investigation in animal brains of ApoE-TR mice corroborates the enhanced eicosanoid signaling with *APOE4* [49]. LTB4 signaling may have a prominent role in inducing oxidative stress. Chuang et al. reported that ROS and NO production during microglia activation is reduced by inhibition of lipoxygenase but not cyclooxygenase [8], suggesting induced LOX signaling as the primary driver of oxidative stress.

Activation of cPLA2 may differ by cell type and within cellular compartments. Recently, astrocytic activation of cPLA2 bound directly with MAVS enhanced NF-κB pathways to produce proinflammatory factors such as Ccl2 and Nos2 in an animal model of multiple sclerosis (MS) [7]. The fact that we did not observe greater CcL2 or Nos2 expression in *APOE4* astrocytes, mouse, or human brains in our current study suggests the selective activation cPLA2 by location within the astrocyte leading to a distinct neuroinflammatory phenotype. In addition to MS, the increase in AA release and its metabolism to prostaglandins and leukotrienes have been observed in cancers and other neurodegeneration diseases [50-52]. For example, *PIK3CA* mutant breast cancer tumor cells displayed dramatically elevated AA and eicosanoid levels, promoting tumor cell proliferation [51].

The activation of MAPK system by ApoE4 likely involves complex set of ApoE receptors or signaling pathways. In neurons, ApoE4 was shown to produce greater activating of the MAPK/ERK system (isoform dependent manner) to induce greater production of APP[53], however, it was not clear if this activation involved ApoE signaling receptors (e.g., ApoER2 and VLDLR) or metabolic receptors (e.g., LRP1 and LDLR). Further studies are needed to sort out the receptor(s) involved in different cell types. That could help elucidate the physiological and pathological pathways relevant to ApoE and/or the receptors and their effect of P38-cPLA2 signaling.

Activation of cPLA2 activity is associated with its phosphorylation [10]. cPLA2 phosphorylation is regulated by ERKs and p38 MAPK pathways, which phosphorylates cPLA2 at Ser-505 and increases its enzymatic activity [9]. cPLA2 phosphorylation and AA release in response to PMA and ATP stimulation in mouse astrocytes are mediated by ERKs and p38 MAPK pathways [10]. In the platelets, cPLA2

phosphorylation was induced by p38 MAPK activation [24]. Here, we found that ApoE4 selectively activated p38 but not ERKs, and inhibition of p38 in ApoE4 astrocytes decreased cPLA2 activation. This activation of p38 is consistent with a previous report of greater p38 activation but not ERKs pathway in ApoE4-TR mice [54]. Interestingly, p38 inhibitors are in drug development pipelines for AD [55].

Our study has strengths and some limitations. We confirmed our findings of greater cPLA2 activation in several independent models: primary cells, synaptosomes, in ApoE-TR animal models, and in human brains matched by disease stage and differing by genotype. We identified the signaling pathway involved in cPLA2 activation- (MAPK-p38) and validated this in both animal and human brains. Some of the limitations include not examining the effects of ApoE4 on cPLA2 activation on microglia. It is plausible that ApoE4 enhances microglial activation through a cPLA2 dependent mechanism, with unique downstream activation patterns. In the clinical cohort, we did not study cPLA2 expression in *APOE4* homozygote patients without cognitive impairment, as this condition is infrequent. We also acknowledge that the small sample sizes the human brain cohort that can preclude the full examination of the effect of sex on the association between *APOE4* and neuroinflammation. Future studies will include larger sample sizes and more specific approaches (such as single-cell sequencing) to capture cPLA2's activation fingerprint on different brain cell types.

Conclusions

Overall, using multiple approaches, our study has identified that the activation of cPLA2 is implicated in neuroinflammation and oxidative stress associated with *APOE4* (Fig 10). Our findings support the induction of the MAPK-p38 pathway as the driving factor for the activation of the cPLA2-LTB4 signaling cascade, and our cellular studies prioritize astrocytes as the target cell type. Small molecular inhibitors of cPLA2 can be tested *in vivo* for their capacity to reduce the risk of AD dementia associated with carrying the *APOE4* allele.

Materials And Methods

Clinical Samples

The frozen hippocampi of AD patients with *APOE4/E4* carriers (N=9) and no-cognitive impairment (NCI) with *APOE3/E3* carriers (N=7) were collected from the University of Southern California (USC) Alzheimer Disease Research Center (ADRC) Neuropathology core, which was approved by USC's Institutional Review Board (IRB) protocol (HS-16-00888). The frozen inferior frontal lobe (Brodmann area 10) of the individuals with NCI and the *APOE3/E3* carriers (N=12) and *APOE3/E4* carriers (N=10) and persons with AD patients and the *APOE3/E3* (N=12) and *APOE3/E4* genotypes (N=10) were obtained from the Rush Alzheimer's Disease Center (RADC) at the Rush University Medical Center. Rush Memory and Aging Project was approved by an Institutional Review Board (IRB) of Rush University Medical Center.

Animals

ApoE3-TR and ApoE4-TR mice were a generous gift from Dr. Patrick Sullivan. The endogenous mouse ApoE was replaced by either human APOE3 or APOE4, created by gene targeting, as described previously [56]. All experiments were performed on age-matched male animals (8 months of age) and were approved by the USC Animal Care Committee. Every effort was made to reduce animal stress and to minimize animal usage. The mice were anesthetized with isoflurane and perfused with PBS. The brains were split in half for further analysis.

Cell cultures

Primary astrocytes were obtained from C57JB6, ApoE3-TR, and ApoE4-TR mice pups and cultured, as described previously[57]. Briefly, cerebral cortices from each 1 to 3 day-old neonatal mouse were dissected in ice-cold Hanks' Balanced Salt Solution (HBSS) (Corning, 21-021-CV) and digested with 0.25% trypsin for 20min at 37°C. Trypsinization was stopped by the addition of a 2-fold volume of DMEM (Corning, 10-013) with 10% fetal bovine serum (FBS) (Omega Scientific, FB-12) and 1% antibiotic-antimycotic (Anti-anti) (Thermo Fisher, 15240062). The cells were dispersed into a single-cell level by repeated pipetting and filtered through 100mm cell strainers (VWR, 10199-658). After filtering, cells were centrifuged for 5 min at 1000 rpm and resuspended in a culture medium supplemented with 10% FBS and antibiotics. Then, cells were seeded in a 75 cm^2 flask and cultured at 37°C in 5% CO2. The medium was changed on the next day and then replaced every 3 days. These mixed glia cultures reached confluence after 7–10 days. The cells were then shaken at 250 rpm for 16h at 37°C to remove microglia and oligodendrocyte progenitor cells. The remaining cells were harvested by digestion with trypsin. At this stage, the culture contained 95% astrocytes and was used for further experiments.

Immortalized mouse astrocytes derived from human ApoE3 and ApoE4 knock-in mice [58] were gifts from Dr. David Holtzman and grown in DMEM/F12 (Corning, MT10090CV) containing 10% FBS, 1mM sodium pyruvate (Thermo Fisher, 11360070), 1mM geneticin (Thermo Fisher, 10131-035) and 1% anti-anti.

Cell lysate and brain homogenate preparation

The immortalized or primary astrocytes were lysed with 1x RIPA buffer (Cell Signaling Technology, CST 9806) containing protease inhibitor cocktail (Sigma, P8340) and phosphatase inhibitor cocktail (Sigma, P0044), followed by centrifugation at 14,000 gs for 10 min at 4 °C. The supernatant was collected for further analysis.

The mouse cerebral cortex, human hippocampus, and inferior frontal cortex were weighed, then RIPA buffer containing protease inhibitor cocktail and phosphatase inhibitor cocktail was added as 1:30 (w/v). The tissue was then homogenized using a 2 mL glass Dounce tissue grinder, followed by centrifugation with 14,000 gs for 10 min at 4 °C. The supernatant was collected, and the concentration was measured by BCA kit.

cPLA2 protein enrichment

To detect the phosphorylated cPLA2 in mouse cortex homogenates, cPLA2 protein was enriched by immunoprecipitation. For each mouse sample, 5 µg of cPLA2 antibody (Santa Cruz Biotechnology, sc-376618) was conjugated to 50 µL Dynabeads Protein G (Thermo Scientific, 10003D) for 1 hr at room temperature, then 500 µg total protein in 500µL RIPA was added to the cPLA2-beads complex and incubated with rotation overnight at 4 °C. The beads were washed with 0.1% PBST 3 times by rotation for 5 min. After washing, 30µL of 1x sample buffer (Bio-Rad, 1610747) was added to the beads and heated for 10 minutes at 100°C. The supernatant was collected by magnetic force and used for the further Western-blot assay.

Western-blot

The cell lysates, cortex homogenate, and enriched cPLA2 proteins were separated by 4–15% mini-precast protein gels (Bio-Rad, 4561086) under reducing conditions and then transferred onto nitrocellulose membranes (Bio-Rad, 1704270). After transfer, membranes were blocked with 5% fat-free milk (Bio-Rad, 1706404) in TBST for 1 h at room temperature, followed by overnight incubation with the primary antibody in 5% BSA at 4°C. Then, the membranes were incubated with HRP conjugated secondary antibody for 1 h at room temperature. Chemiluminescent HRP substrate (Millipore, WBKLS0500) was used for detection. Fujifilm LAS-4000 imager system was used to capture images, and the densitometric quantification was done by Gel Quant NET software.

The following antibodies and dilution factors were used: cPLA2 antibody (Santa Cruz Biotechnology, sc-376618) (1:200), phospho-cPLA2 (Ser505) antibody (CST, 53044) (1:1000), phospho-ERK1/2 antibody (CST, 4370) (1:1000), ERK1/2 antibody (CST, 4595) (1:1000), p38 antibody (CST, 9212) (1:1000), phospho-p38 antibody (CST, 4511) (1:1000), GFAP antibody (CST, 12389) (1:1000), Iba-1 antibody (GeneTex, GTX100042) (1:1000), iNOS antibody (CST, 13120) (1:1000), β-actin antibody (CST, 3700) (1:1000), β-tubulin antibody (CST, 2146) (1:1000), HRP-linked anti-mouse IgG (CST, 7076) (1:2000), HRP-linked anti-rabbit IgG (CST, 7074) (1:2000).

qPCR

The cells and brain specimens were harvested, and RNA was extracted using an RNA extraction kit (Thermo Fisher, K0731). Synthesis of cDNA was done using High-Capacity cDNA Reverse Transcription Kit (Thermo Fisher, 4368814). qPCR was performed using the PowerUp SYBR Green Master Mix (Thermo Fisher, A25742). The following primers were synthesized by Integrated DNA Technologies. The cPLA2 sense (5'-CTGCAAGGCCGAGTGACA-3') and antisense (5'-TTCGCCCACTTCTCTGCAA-3'); mouse Tnfa sense (5'-GCCTCTTCTCATTCCTGCTTG-3') and antisense (5'-CTGATGAGAGGGAGGCCATT-3'); mouse Il1b sense (5'-GCAACTGTTCCTGAACTCAACT-3') and antisense (5'-ATCTTTTGGGGTCCGTCAACT-3'); mouse Il6 sense (5'-TAGTCCTTCCTACCCCAATTTCC-3') and antisense (5'-TTGGTCCTTAGCCACTCCTTC-3'); mouse Ccl2 sense (5'-GTCCCTGTCATGCTTCTGG-3') and antisense (5'-GCTCTCCAGCCTACTCATTG-3'); mouse Mip1a sense (5'- TGAAACCAGCAGCCTTTGCTC-3') and antisense (5'-AGGCATTCAGTTCCAGGTCAGTG-3'); mouse Mip2 sense (5'-ATCCAGAGCTTGAGTGTGACGC-3') and antisense (5'- AAGGCAAACTTTTTGACCGCC-3'); mouse b-actin sense (5'-ACCTTCTACAATGAGCTGCG-3') and antisense (5'-CTGGATGGCTACGTACATGG-3'); human TNFa sense (5'-ACTTTGGAGTGATCGGCC-3') and antisense (5'-GCTTGAGGGTTTGCTACAAC-3'); human IL1b sense (5'-ATGCACCTGTACGATCACTG-3') and antisense (5'-ACAAAGGACATGGAGAACACC-3');

human IL6 sense (5'-CCACTCACCTCTTCAGAACG-3') and antisense (5'-CATCTTTGGAAGGTTCAGGTTG-3'); human CCL2 sense (5'- TGTCCCAAAGAAGCTGTGATC-3') and antisense (5'-ATTCTTGGGTTGTGGAGTGAG-3'); human GAPDH sense (5'-ACATCGCTCAGACACCATG-3') and antisense (5'-TGTAGTTGAGGTCAATGAAGGG-3')

AA and DHA efflux assays

To investigate arachidonic acid (AA) and docosahexaenoic acid (DHA) release by cPLA2 and iPLA2 activation, respectively, we performed an AA and DHA efflux assay as described previously [2]. ApoE3 and ApoE4 primary astrocytes were seeded at 5000 cells/well in 96-well plates. After 24 h, the culture medium was changed with serum-free DMEM containing fatty acid-free BSA (5mg/mL) (Sigma, A9647) and ^{3}H-AA (1μCi/mL) or ^{14}C-DHA (1μCi/mL) (Moravek) for 24h. The cells were then washed twice with 100 μL of DMEM, and 100 μL of DMEM containing BSA (5mg/mL) was added. After 30 minutes, the medium was removed, and 100μL of ATP (100μM) in DMEM without BSA was added. After 15 minutes, the cell culture medium was collected and transferred to scintillation vials filled with 3mL of scintillation cocktail. The cells were solubilized in 90 μL of NaOH (0.5N) for 5 minutes, neutralized with 60 μL PBS, and then transferred to scintillation vials filled with 3mL scintillation cocktail. After rigorous mixing, the vials were counted in a Beckman LS6500 liquid scintillation counter (Beckman Coulter). The efflux of AA and DHA were assessed by the ratio of the corresponding fatty acid in the medium to total (medium and cell lysate). The change of AA and DHA efflux was calculated by subtracting the levels of AA and DHA in the ATP treated group to ATP non-treated group for each genotype. WT primary astrocytes were plated and labeled with ^{3}H-AA (1μCi/mL) or ^{14}C-DHA (1μCi/mL) as described above. Then, the cells were washed twice with 100μL of DMEM. After wash, 10μL of DMEM containing BSA and 0.2 μM recombinant ApoE3

or ApoE4 protein were added. After 24 h, the medium was removed, and 100µL of ATP (100 µM) in DMEM without BSA was added. The AA and DHA efflux were measured as described above after 15 minutes.

cPLA2 activity assay

cPLA2 activity was detected by the cPLA2 activity assay kit (Cayman Chemical, 765021). The mouse cortex was homogenized into HEPES buffer (50mM, pH 7.4, containing 1mM EDTA) as 1:10 (w/v), and the supernatant was collected after centrifuged and used for cPLA2 activity detection.

Immunoprecipitation

Immortalized ApoE4 astrocytes were cultured in a 100-mm dish for 18 hours and then were lysed with RIPA containing protease and phosphatase inhibitors. The lysates were used for immunoprecipitation with an anti-cPLA2 antibody or species-matched IgG. After elution, cPAL2 and p38 were detected by Western-blot.

p38 MAPK inhibiton experiment

ApoE4 primary astrocytes were seeded in a 24-wells plate with the intensity of 100,000 cells per well. Forty-eight hours later, cells were pre-treated with p38 MAPK inhibitors – SB202190 (10µM, Sigma, S7076) or SB203580 (10µM, Sigma, S8307) in the DMEM culture medium without FBS for 20 minutes, followed by the treatment with vehicle or TNFa (10ng/mL) (R&D Systems, 210-TA-005) plus IFNg (100ng/mL) (Sigma, SRP3058) together for 30 minutes. Then, the cells were lysed with RIPA. Total and phosphorylated cPLA2 and p38 were detected by Western-blot.

LTB4 and PGE2 measurement

For the LTB4 and PGE2 measurements in the human brain samples, brain tissue was weighed, then PBS containing 1 mM EDTA, 10 µM indomethacin (Cox inhibitor, Sigma I8280), and 10 µM NDGA (Lox inhibitor, Sigma 479975) as 1:10 (w/v) were added. The tissue was then homogenized using a 2mL glass Dounce tissue grinder, followed by centrifugation with 8,000 x g for 10 minutes at 4 °C. The supernatant was collected, and the protein concentration was measured using a BCA kit. LTB4 and PGE2 levels were detected by the assay kit (LTB4 ELISA Kit, Cayman Chemical, 10009292; PGE2 ELISA Kit, Cayman Chemical, 500141).

For the LTB4 measurement in the cells, ApoE3 and ApoE4 primary astrocytes were seeded in a 24-wells plate with the intensity of 100,000 cells per well. Forty-eight hours later, cells were pre-treated with cPLA2 inhibitor-Pyrrophenone (500nM, Sigma, 5305380001) in the DMEM culture medium without FBS but containing N2 supplement for 30 minutes, followed by the treatment with vehicle or TNFa (10ng/mL) (R&D Systems, 210-TA-005) plus IFNg (100ng/mL) (Sigma, SRP3058) together for 18 hours. Then, the culture media and cell lysate were collected. LTB4 levels were measured in a 4-fold concentrated medium using the assay kit.

ApoE4 primary astrocytes were seeded in a 24-wells plate with the intensity of 100,000 cells per well. Forty-eight hours later, cells were transfected with cPLA2 or non-target (NT) siRNA (10nM) for 48 hours, followed by the treatment with vehicle or TNFa (10ng/mL) plus IFNg (100ng/mL) together for 24 hours. Then, the culture media and cell lysate were collected. LTB4 levels were measured in a 4-fold concentrated medium by the assay kit.

ROS measurement

ROS were detected by the DCFDA cellular ROS detection assay kit (Abcam, ab113851). ApoE3 and ApoE4 primary astrocytes were seeded in dark, clear bottom 96-wells plate with the intensity of 20,000 cells per well. Forty-eight hours later, cells were pre-treated with cPLA2 inhibitor (1μM) in the DMEM culture medium without FBS but containing N2 supplement for 30 minutes, followed by the treatment with vehicle or TNFa (10ng/mL) plus IFNg (100ng/mL) together for 24 hours. After removing the media and washing plate once with 1x assay buffer, the cells were stained with DCFDA solution (100μL/well) for 45 minutes at 37°C in the dark. Then, the DCFDA solution was removed, and the 1x assay buffer (100μL/well) was added to the plate. ROS levels were measured using a fluorescent plate reader at Excision/Emission=485/585nm.

Assessment of activation and cellular distribution of cPLA2 in synaptosomes

Synaptosomes prepared from postmortem human frontal cortices using an established method with minor modification[59]. Briefly, thawed postmortem human frontal cortical slices (about 20 mg) were homogenized in 10 volume of ice-cold homogenization buffer (10 mM HEPES, pH 7.4, 0.32 M sucrose, 0.1 mM EDTA containing EDTA-free protease inhibitor cocktail (Roche, 04693159001) and 0.2% 2-mercaptoethanol) using a Teflon/glass homogenizer (10 strokes). The homogenates were cleared by centrifugation (1000 x g for 10 min), and the supernatants were centrifuged at 15,000 x g at 4°C for 30 min to pellet the synaptosomes (P2 fraction). The synaptosomes were washed twice at 4°C in 1 mL of ice-cold oxygenated K-R (Kreb's-Ringer) solution (25 mM HEPES, pH 7.4, 118 mM NaCl, 4.8 mM KCl, 25 mM $NaHCO_3$, 1.3 mM $CaCl_2$, 1.2 mM $MgSO_4$, 1.2 mM KH_2PO_4, 10 mM glucose, 100 μM ascorbic acid, EDTA-free protease inhibitor cocktail). The synaptosomes were then resuspended in 1 mL of K-R solution,

and the protein concentrations were determined by the BCA kit. Two hundred µg synaptosomes were incubated with 0.1 µM of Aβ42, rApoE3, rApoE4 or Aβ42+rApoE4 in 200 µL oxygenated Kreb's-Ringer for 30 min at 37°C followed by incubation with 1 µM A23187 (Santa Cruz Biotechnology, sc-3591), 5 ng/mL TNFα+ 10 ng/mL IFN or 2.5 µM ceramide-1-phosphate (Sigma, C4832) for 15 min (oxygenated with 95% O2/5% CO2 for 1 min every 10 min). Upon completion of incubation, an ice-cold protein phosphatase inhibitor cocktail (Roche, 04906837001) is added and placed on ice for 5 min, and synaptosomes were pelleted by centrifugation.

The cytosolic and membranous fractions of the synaptosomes were prepared as established previously with minor modifications [60]. The synaptosomes were briefly sonicated (Kontes Micro Cell Disrupter) in 250 µL of immunoprecipitation buffer (25 mM HEPES, pH 7.5, 200 mM NaCl, 1 mM EDTA, protease and protein phosphatase inhibitor cocktails, and 0.02% 2-mercaptoethanol and centrifuged at 48,000 x g for 15 min. The resultant supernatant was removed as the cytosolic fraction, and the pellet was briefly sonicated in 200 µL immunoprecipitation buffer as the membranous fraction. Both cytosolic and membranous fractions were solubilized with 0.5% digitonin, 0.2% sodium cholate, and 0.5% NP-40 (total incubation volume was 220 µL and incubated at 4°C with end-to-end shaking for 1 h. After dilution with 780 µL of ice-cold immunoprecipitation buffer and centrifugation (4°C) to remove insoluble debris. cPLA2 were isolated by immunoprecipitation with 16 h incubation at 4°C with anti-cPLA2 antibodies (Santa Cruz Biotechnology, sc-376618, and sc-137069) and protein A/G-conjugated agarose beads (Thermo Fisher, 20432). The resultant immunocomplexes were pelleted by centrifugation at 4°C. After three washes with 1 mL of ice-cold PBS, pH 7.2, and centrifugation, the isolated cPLA2 was eluted with 90 µl IgG elution buffer (Thermo Fisher, 21004), neutralized by 10 µL 1.5 M Tris-HCl (pH9.0) and then solubilized by boiling for 5 min with 17 µL of 6X SDS-PAGE sample preparation buffer. The contents of activated cPLA2 (p-cPLA2) and total cPLA2 in 50% of the obtained anti-cPLA2 immunoprecipitants were determined respectively by Western-blot with anti-phosphorylated cPLA2 (Cell Signaling Technologies, 53044) and anti-cPLA2 (Santa Cruz Biotechnology, sc-376618) antibodies.

Statistical analysis

Descriptive results are presented as the mean ± SD. Data were analyzed using Student's unpaired t-test or ANOVA. The cPLA2 phosphorylation was compared in APOE groups using a linear regression model, adjusting for age, sex, and Braak stage. Non-parametric tests were used for non-normally distributed data. Statistical significance was present at $p<0.05$. Statistical program R, version 3.5 was used. Quantification of WB gels was conducted on three independent experiments.

Abbreviations

ApoE, Apolipoprotein E; ApoE-TR, ApoE-targeted replacement; AD, Alzheimer disease; NCI, no cognitive impairment; cPLA2, calcium-dependent cytosolic phospholipase A2; iPLA2, calcium-independent phospholipase A2 (iPLA2); DHA, docosahexaenoic acid; AA, arachidonic acid; LPC, lysophosphatidylcholine; LTB4, leukotriene B4; PGE2, prostaglandin E2; ROS, reactive oxygen species;

iNOS, inducible nitric oxide synthase; NO, nitric oxide; COX, cyclooxygenase; LOX, lipoxygenase; MAPK, mitogen-activated protein kinase; MAVS, mitochondrial antiviral-signaling protein; NF-kB; nuclear factor kappa-light-chain-enhancer of activated B cells; LPS, lipopolysaccharide; CRP, C reactive protein.

Declarations

Ethics approval and consent to participate

The frozen hippocampus samples were collected from the University of Southern California (USC) Alzheimer Disease Research Center (ADRC) Neuropathology core, which was approved by USC's Institutional Review Board (IRB) protocol (HS-16-00888). The frozen inferior frontal lobe (Brodmann area 10) were obtained from the Rush Alzheimer's Disease Center (RADC) at the Rush University Medical Center. Rush Memory and Aging Project was approved by an Institutional Review Board (IRB) of Rush University Medical Center.

The USC Animal Care Committee approved the mouse studies.

Consent for publication

Not applicable.

Availability of data and materials

All data used and analyzed for the current study are available from the corresponding author on reasonable request.

Competing interests

The authors declare that they have no competing interests.

Funding

HNY was supported by R21AG056518, R01AG055770, R01AG054434, R01AG067063 from the National Institute on Aging. This work was also supported by P50AG05142 (HCC), P30 AG10161 (DAB), R01 AG17917 (DAB), R01 NS084965 (ZA), and RF1 AG059621 (ZA) from the National Institutes of Health. The contribution of SIR was funded by the Intramural Program of the National Institute on Alcohol Abuse and Alcoholism. Funders had no role in study design, data collection, data analysis, interpretation, or writing of the report.

Authors' contributions

HNY and SW designed experiments. SW and BL performed experiments. SW wrote the manuscript. PMS supplied mice. DAB and ZA supplied human cortex samples. HCC and CM supplied human hippocampus

samples. HYW conducted the synaptosome experiments. VS, AF, SIR, DAB, ZA, HC, CM, HWY and HNY revised manuscript.

Acknowledgments

We thank Dr. Caleb Finch for critically reviewing the manuscript. We thank Dr. David M. Holtzman for providing us with ApoE3 and ApoE4 immortalized astrocytes.

References

1. Six DA, Dennis EA: **The expanding superfamily of phospholipase A2 enzymes: classification and characterization.** *Biochimica et Biophysica Acta (BBA)-Molecular and Cell Biology of Lipids* 2000, **1488:**1-19.
2. Strokin M, Sergeeva M, Reiser G: **Docosahexaenoic acid and arachidonic acid release in rat brain astrocytes is mediated by two separate isoforms of phospholipase A2 and is differently regulated by cyclic AMP and Ca2+.** *Br J Pharmacol* 2003, **139:**1014-1022.
3. Cheon Y, Kim H-W, Igarashi M, Modi HR, Chang L, Ma K, Greenstein D, Wohltmann M, Turk J, Rapoport SI: **Disturbed brain phospholipid and docosahexaenoic acid metabolism in calcium-independent phospholipase A2-VIA (iPLA2β)-knockout mice.** *Biochimica et Biophysica Acta (BBA)-Molecular and Cell Biology of Lipids* 2012, **1821:**1278-1286.
4. Gijón MA, Leslie CC: **Regulation of arachidonic acid release and cytosolic phospholipase A2 activation.** *Journal of leukocyte biology* 1999, **65:**330-336.
5. Berk P, Stump D: **Mechanisms of cellular uptake of long chain free fatty acids.** In *Lipid Binding Proteins within Molecular and Cellular Biochemistry.* Springer; 1999: 17-31
6. Leslie CC: **Cytosolic phospholipase A2: physiological function and role in disease.** *Journal of lipid research* 2015, **56:**1386-1402.
7. Chao CC, Gutierrez-Vazquez C, Rothhammer V, Mayo L, Wheeler MA, Tjon EC, Zandee SEJ, Blain M, de Lima KA, Takenaka MC, et al: **Metabolic Control of Astrocyte Pathogenic Activity via cPLA2-MAVS.** *Cell* 2019, **179:**1483-1498 e1422.
8. Chuang DY, Simonyi A, Kotzbauer PT, Gu Z, Sun GY: **Cytosolic phospholipase A 2 plays a crucial role in ROS/NO signaling during microglial activation through the lipoxygenase pathway.** *Journal of neuroinflammation* 2015, **12:**199.
9. Lin L-L, Wartmann M, Lin AY, Knopf JL, Seth A, Davis RJ: **cPLA2 is phosphorylated and activated by MAP kinase.** *Cell* 1993, **72:**269-278.
10. Xu J, Weng Y-I, Simonyi A, Krugh BW, Liao Z, Weisman GA, Sun GY: **Role of PKC and MAPK in cytosolic PLA2 phosphorylation and arachadonic acid release in primary murine astrocytes.** *J Neurochem* 2002, **83:**259-270.
11. Perez-Nievas BG, Stein TD, Tai H-C, Dols-Icardo O, Scotton TC, Barroeta-Espar I, Fernandez-Carballo L, De Munain EL, Perez J, Marquie M: **Dissecting phenotypic traits linked to human resilience to**

Alzheimer's pathology. *Brain* 2013, **136:**2510-2526.

12. Stephenson DT, Lemere CA, Selkoe DJ, Clemens JA: **Cytosolic phospholipase A2 (cPLA2) immunoreactivity is elevated in Alzheimer's disease brain.** *Neurobiology of disease* 1996, **3:**51-63.
13. Colangelo V, Schurr J, Ball MJ, Pelaez RP, Bazan NG, Lukiw WJ: **Gene expression profiling of 12633 genes in Alzheimer hippocampal CA1: transcription and neurotrophic factor down-regulation and up-regulation of apoptotic and pro-inflammatory signaling.** *Journal of neuroscience research* 2002, **70:**462-473.
14. Sanchez-Mejia RO, Newman JW, Toh S, Yu GQ, Zhou Y, Halabisky B, Cisse M, Scearce-Levie K, Cheng IH, Gan L, et al: **Phospholipase A2 reduction ameliorates cognitive deficits in a mouse model of Alzheimer's disease.** *Nat Neurosci* 2008, **11:**1311-1318.
15. Sun GY, He Y, Chuang DY, Lee JC, Gu Z, Simonyi A, Sun AY: **Integrating cytosolic phospholipase A 2 with oxidative/nitrosative signaling pathways in neurons: a novel therapeutic strategy for AD.** *Molecular neurobiology* 2012, **46:**85-95.
16. Palavicini JP, Wang C, Chen L, Hosang K, Wang J, Tomiyama T, Mori H, Han X: **Oligomeric amyloid-beta induces MAPK-mediated activation of brain cytosolic and calcium-independent phospholipase A 2 in a spatial-specific manner.** *Acta neuropathologica communications* 2017, **5:**56.
17. Sundaram JR, Chan ES, Poore CP, Pareek TK, Cheong WF, Shui G, Tang N, Low C-M, Wenk MR, Kesavapany S: **Cdk5/p25-induced cytosolic PLA2-mediated lysophosphatidylcholine production regulates neuroinflammation and triggers neurodegeneration.** *Journal of Neuroscience* 2012, **32:**1020-1034.
18. Qu B, Gong Y, Gill JM, Kenney K, Diaz-Arrastia R: **Heterozygous knockout of cytosolic phospholipase A2α attenuates Alzheimer's disease pathology in APP/PS1 transgenic mice.** *Brain research* 2017, **1670:**248-252.
19. Tao Q, Ang TFA, DeCarli C, Auerbach SH, Devine S, Stein TD, Zhang X, Massaro J, Au R, Qiu WQ: **Association of Chronic Low-grade Inflammation With Risk of Alzheimer Disease in ApoE4 Carriers.** *JAMA Netw Open* 2018, **1:**e183597.
20. Ramassamy C, Averill D, Beffert U, Theroux L, Lussier-Cacan S, Cohn JS, Christen Y, Schoofs A, Davignon J, Poirier J: **Oxidative insults are associated with apolipoprotein E genotype in Alzheimer's disease brain.** *Neurobiology of disease* 2000, **7:**23-37.
21. Tomaszewski N, He X, Solomon V, Lee M, Mack WJ, Quinn JF, Braskie MN, Yassine HN: **Effect of APOE Genotype on Plasma Docosahexaenoic Acid (DHA), Eicosapentaenoic Acid, Arachidonic Acid, and Hippocampal Volume in the Alzheimer's Disease Cooperative Study-Sponsored DHA Clinical Trial.** *J Alzheimers Dis* 2020, **74:**975-990.
22. Yassine HN RV, Mack WJ, Quinn JF, Yurko-Mauro K, Bailey-Hall E, Aisen PS, Chui HC, Schneider LS: **The effect of APOE genotype on the delivery of DHA to cerebrospinal fluid in Alzheimer's disease.** *Alzheimer's Reaserch and Therapy* 2016, **8:**25.
23. Moore SA: **Polyunsaturated fatty acid synthesis and release by brain-derived cells in vitro.** *Journal of Molecular Neuroscience* 2001, **16:**195-200.

24. Kramer RM, Roberts EF, Um SL, Borsch-Haubold AG, Watson SP, Fisher MJ, Jakubowski JA: **p38 mitogen-activated protein kinase phosphorylates cytosolic phospholipase A2 (cPLA2) in thrombin-stimulated platelets. Evidence that proline-directed phosphorylation is not required for mobilization of arachidonic acid by cPLA2.** *J Biol Chem* 1996, **271:**27723-27729.

25. Yun B, Lee H, Jayaraja S, Suram S, Murphy RC, Leslie CC: **Prostaglandins from Cytosolic Phospholipase A2α/Cyclooxygenase-1 Pathway and Mitogen-activated Protein Kinases Regulate Gene Expression in Candida albicans-infected Macrophages.** *The Journal of biological chemistry* 2016, **291:**7070-7086.

26. Kumar S, Jiang MS, Adams JL, Lee JC: **Pyridinylimidazole compound SB 203580 inhibits the activity but not the activation of p38 mitogen-activated protein kinase.** *Biochemical and biophysical research communications* 1999, **263:**825-831.

27. Bate C, Williams A: **Monomeric amyloid-β reduced amyloid-β oligomer-induced synapse damage in neuronal cultures.** *Neurobiology of disease* 2018, **111:**48-58.

28. Vitek MP, Brown CM, Colton CA: **APOE genotype-specific differences in the innate immune response.** *Neurobiol Aging* 2009, **30:**1350-1360.

29. Colton CA, Brown CM, Cook D, Needham LK, Xu Q, Czapiga M, Saunders AM, Schmechel DE, Rasheed K, Vitek MP: **APOE and the regulation of microglial nitric oxide production: a link between genetic risk and oxidative stress.** *Neurobiology of aging* 2002, **23:**777-785.

30. Guo L, LaDu MJ, Van Eldik LJ: **A dual role for apolipoprotein e in neuroinflammation: anti- and pro-inflammatory activity.** *J Mol Neurosci* 2004, **23:**205-212.

31. Chen S, Averett NT, Manelli A, Ladu MJ, May W, Ard MD: **Isoform-specific effects of apolipoprotein E on secretion of inflammatory mediators in adult rat microglia.** *J Alzheimers Dis* 2005, **7:**25-35.

32. Shi Y, Yamada K, Liddelow SA, Smith ST, Zhao L, Luo W, Tsai RM, Spina S, Grinberg LT, Rojas JC, et al: **ApoE4 markedly exacerbates tau-mediated neurodegeneration in a mouse model of tauopathy.** *Nature* 2017, **549:**523-527.

33. Tai LM, Balu D, Avila-Munoz E, Abdullah L, Thomas R, Collins N, Valencia-Olvera AC, LaDu MJ: **EFAD transgenic mice as a human APOE relevant preclinical model of Alzheimer's disease.** *Journal of lipid research* 2017, **58:**1733-1755.

34. Zhu Y, Nwabuisi-Heath E, Dumanis SB, Tai LM, Yu C, Rebeck GW, Ladu MJ: **APOE genotype alters glial activation and loss of synaptic markers in mice.** *Glia* 2012, **60:**559-569.

35. Ophir G, Amariglio N, Jacob-Hirsch J, Elkon R, Rechavi G, Michaelson DM: **Apolipoprotein E4 enhances brain inflammation by modulation of the NF-κB signaling cascade.** *Neurobiology of disease* 2005, **20:**709-718.

36. Gale SC, Gao L, Mikacenic C, Coyle SM, Rafaels N, Dudenkov TM, Madenspacher JH, Draper DW, Ge W, Aloor JJ: **APOε4 is associated with enhanced in vivo innate immune responses in human subjects.** *Journal of allergy and clinical immunology* 2014, **134:**127-134. e129.

37. Montine KS, Olson SJ, Amarnath V, Whetsell WO, Jr., Graham DG, Montine TJ: **Immunohistochemical detection of 4-hydroxy-2-nonenal adducts in Alzheimer's disease is associated with inheritance of**

APOE4. *Am J Pathol* 1997, **150:**437-443.

38. Egensperger R, Kösel S, von Eitzen U, Graeber MB: **Microglial activation in Alzheimer disease: association with APOE genotype.** *Brain Pathology* 1998, **8:**439-447.
39. Minett T, Classey J, Matthews FE, Fahrenhold M, Taga M, Brayne C, Ince PG, Nicoll JA, Boche D, CFAS M: **Microglial immunophenotype in dementia with Alzheimer's pathology.** *Journal of neuroinflammation* 2016, **13:**135.
40. Friedberg JS, Aytan N, Cherry JD, Xia W, Standring OJ, Alvarez VE, Nicks R, Svirsky S, Meng G, Jun G: **Associations between brain inflammatory profiles and human neuropathology are altered based on apolipoprotein E ε4 genotype.** *Scientific Reports* 2020, **10:**1-10.
41. Fonteh AN, Chiang J, Cipolla M, Hale J, Diallo F, Chirino A, Arakaki X, Harrington MG: **Alterations in cerebrospinal fluid glycerophospholipids and phospholipase A2 activity in Alzheimer's disease.** *Journal of lipid research* 2013, **54:**2884-2897.
42. Esposito G, Giovacchini G, Liow JS, Bhattacharjee AK, Greenstein D, Schapiro M, Hallett M, Herscovitch P, Eckelman WC, Carson RE, Rapoport SI: **Imaging neuroinflammation in Alzheimer's disease with radiolabeled arachidonic acid and PET.** *Journal of nuclear medicine : official publication, Society of Nuclear Medicine* 2008, **49:**1414-1421.
43. Abdullah L, Evans JE, Emmerich T, Crynen G, Shackleton B, Keegan AP, Luis C, Tai L, LaDu MJ, Mullan M: **APOE ε4 specific imbalance of arachidonic acid and docosahexaenoic acid in serum phospholipids identifies individuals with preclinical Mild Cognitive Impairment/Alzheimer's Disease.** *Aging (Albany NY)* 2017, **9:**964.
44. Gentile MT, Reccia M, Sorrentino P, Vitale E, Sorrentino G, Puca A, Colucci-D'Amato L: **Role of cytosolic calcium-dependent phospholipase A2 in Alzheimer's disease pathogenesis.** *Molecular neurobiology* 2012, **45:**596-604.
45. Osborne C, West E, Bate C: **The phospholipase A2 pathway controls a synaptic cholesterol ester cycle and synapse damage.** *J Cell Sci* 2018, **131:**jcs211789.
46. Desbène C, Malaplate-Armand C, Youssef I, Garcia P, Stenger C, Sauvée M, Fischer N, Rimet D, Koziel V, Escanyé M-C: **Critical role of cPLA2 in Aβ oligomer-induced neurodegeneration and memory deficit.** *Neurobiology of aging* 2012, **33:**1123. e1117-1123. e1129.
47. Last V, Williams A, Werling D: **Inhibition of cytosolic phospholipase A 2 prevents prion peptide-induced neuronal damage and co-localisation with beta III tubulin.** *BMC neuroscience* 2012, **13:**106.
48. Sanchez-Mejia RO: **Phospholipase A2 reduction ameliorates cognitive deficits in a mouse model of Alzheimer's disease.** *Nat Neurosci* 2008, **11**.
49. Zhao N, Ren Y, Yamazaki Y, Qiao W, Li F, Felton LM, Mahmoudiandehkordi S, Kueider-Paisley A, Sonoustoun B, Arnold M, et al: **Alzheimer's Risk Factors Age, APOE Genotype, and Sex Drive Distinct Molecular Pathways.** *Neuron* 2020, **106:**727-742.e726.
50. Soubhye J, van Antwerpen P, Dufrasne F: **Targeting Cytosolic Phospholipase A2alpha for Novel Anti-Inflammatory Agents.** *Curr Med Chem* 2018, **25:**2418-2447.

51. Koundouros N, Karali E, Tripp A, Valle A, Inglese P, Perry NJ, Magee DJ, Virmouni SA, Elder GA, Tyson AL: **Metabolic Fingerprinting Links Oncogenic PIK3CA with Enhanced Arachidonic Acid-Derived Eicosanoids.** *Cell* 2020.
52. Vezzani A, Balosso S, Ravizza T: **Neuroinflammatory pathways as treatment targets and biomarkers in epilepsy.** *Nature Reviews Neurology* 2019, **15:**459-472.
53. Huang YA, Zhou B, Wernig M, Sudhof TC: **ApoE2, ApoE3, and ApoE4 Differentially Stimulate APP Transcription and Abeta Secretion.** *Cell* 2017, **168:**427-441.e421.
54. Salomon-Zimri S, Koren A, Angel A, Ben-Zur T, Offen D, Michaelson DM: **The Role of MAPK's Signaling in Mediating ApoE4-Driven Pathology In Vivo.** *Current Alzheimer Research* 2019, **16:**281-292.
55. Scheltens P, Prins N, Lammertsma A, Yaqub M, Gouw A, Wink AM, Chu H-M, van Berckel BNM, Alam J: **An exploratory clinical study of p38α kinase inhibition in Alzheimer's disease.** *Ann Clin Transl Neurol* 2018, **5:**464-473.
56. Sullivan PM, Mezdour H, Aratani Y, Knouff C, Najib J, Reddick RL, Quarfordt SH, Maeda N: **Targeted replacement of the mouse apolipoprotein E gene with the common human APOE3 allele enhances diet-induced hypercholesterolemia and atherosclerosis.** *J Biol Chem* 1997, **272:**17972-17980.
57. Simonovitch S, Schmukler E, Bespalko A, Iram T, Frenkel D, Holtzman DM, Masliah E, Michaelson DM, Pinkas-Kramarski R: **Impaired Autophagy in APOE4 Astrocytes.** *J Alzheimers Dis* 2016, **51:**915-927.
58. Morikawa M, Fryer JD, Sullivan PM, Christopher EA, Wahrle SE, DeMattos RB, O'Dell MA, Fagan AM, Lashuel HA, Walz T, et al: **Production and characterization of astrocyte-derived human apolipoprotein E isoforms from immortalized astrocytes and their interactions with amyloid-beta.** *Neurobiol Dis* 2005, **19:**66-76.
59. Wang H-Y, Stucky A, Liu J, Shen C, Trocme-Thibierge C, Morain P: **Dissociating β-amyloid from α7 nicotinic acetylcholine receptor by a novel therapeutic agent, S 24795, normalizes α7 nicotinic acetylcholine and NMDA receptor function in Alzheimer's disease brain.** *Journal of Neuroscience* 2009, **29:**10961-10973.
60. Wang H-Y, Pisano MR, Friedman E: **Attenuated protein kinase C activity and translocation in Alzheimer's disease brain.** *Neurobiology of aging* 1994, **15:**293-298.

Figures

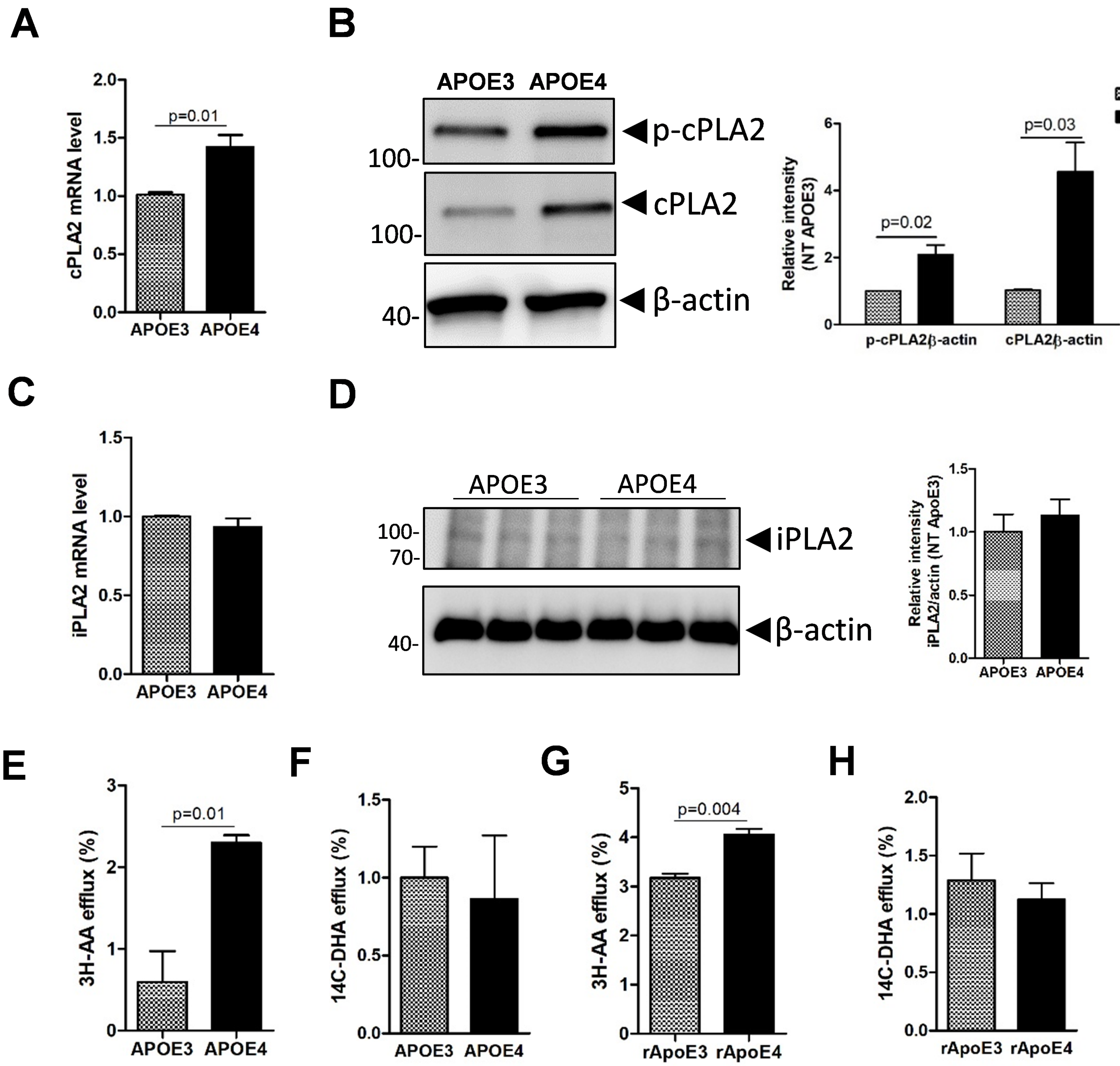

Figure 1

ApoE4 increases cPLA2 but not iPLA2 expression in mouse primary astrocytes. A. cPLA2 mRNA levels in primary astrocytes from APOE3 and APOE4-TR mice. B, cPLA2, and phosphorylated cPLA2 (p-cPLA2) protein levels in primary astrocytes from ApoE3 and ApoE4-TR mice (left) were detected by densitometry (western blot -WB). C, iPLA2 mRNA levels in primary astrocytes from ApoE3 and ApoE4-TR mice. D, iPLA2 protein levels in primary astrocyte cultures from ApoE3 and ApoE4-TR mice (left) was detected by WB. E, F, Primary astrocytes from ApoE3 and ApoE4-TR mice were incubated with 3H-labelled AA (E) or 14C-labeled DHA (F) for 24h, followed by induction by 100nM ATP for 15min. The efflux of 3H-AA (E) and 14C-DHA (F) from cells to media was measured by scintillation counting. G, H, Primary astrocytes from C57BL/6 wild type mice were labeled with 3H-AA (G) or 14C-DHA (H) for 24h and then treated with

recombinant ApoE3 or ApoE4 for 24h, followed by induction with 100nM ATP for 15min. 3H-AA (G) and 14C-DHA (H) efflux were measured by scintillation counting.

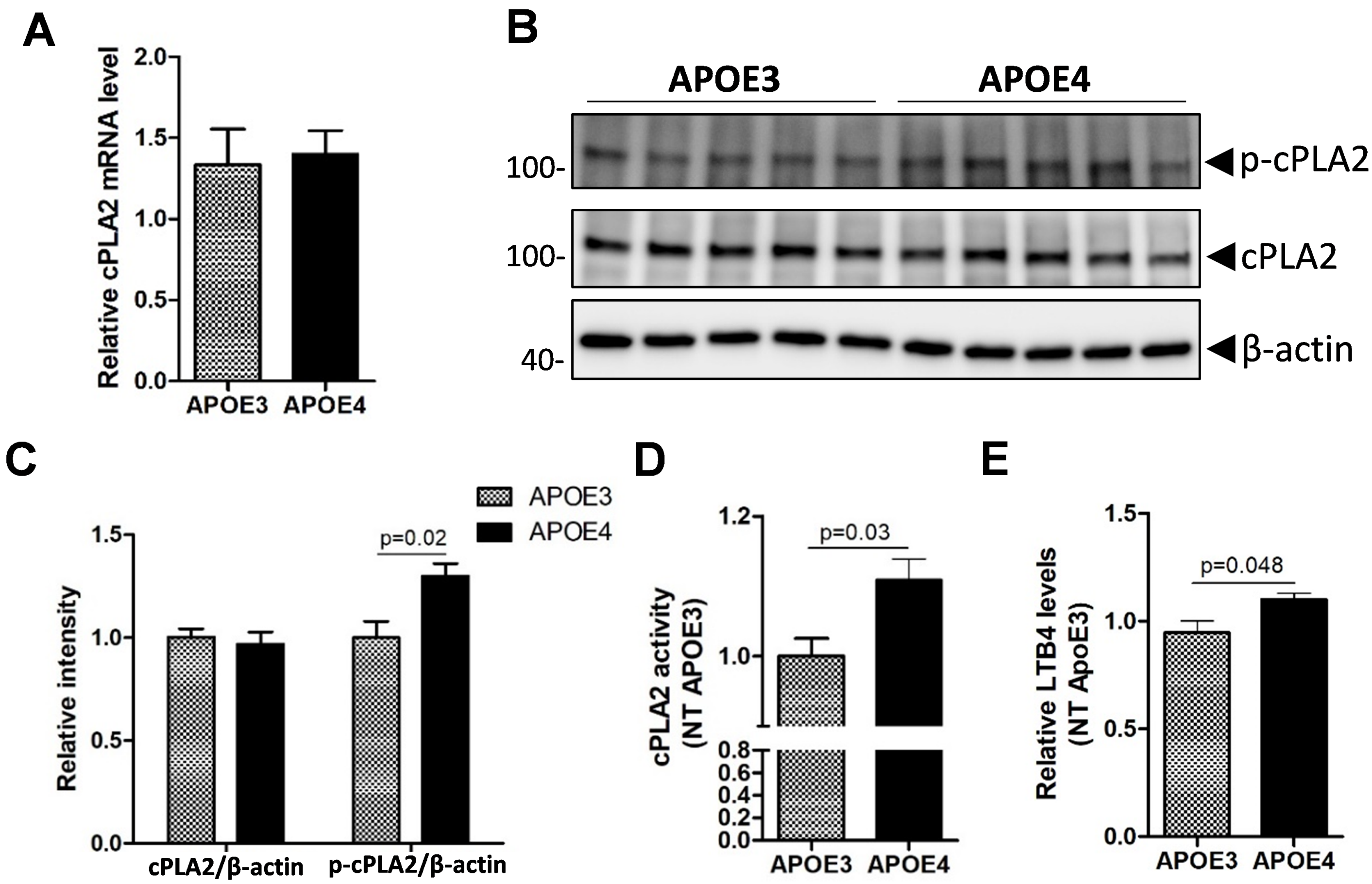

Figure 2

cPLA2 and phosphorylated-cPLA2 level in 8-month old ApoE3-TR and ApoE4-TR mouse brains. The cortex of 8-month old ApoE3 and ApoE4-TR mice were collected. A, cPLA2 mRNA level in the cortex was detected by qPCR. B, phosphorylated-cPLA2 and total cPLA2 protein levels in the cortex were detected by densitometry (western-blot). C. D, cPLA2 activity in mouse cortex homogenates were measured by cPLA2 activity assay kit. E, LTB4 levels in mouse cortical homogenates were measured by LTB4 assay kit. (n=5 for each genotype, 3 males and 2 females).

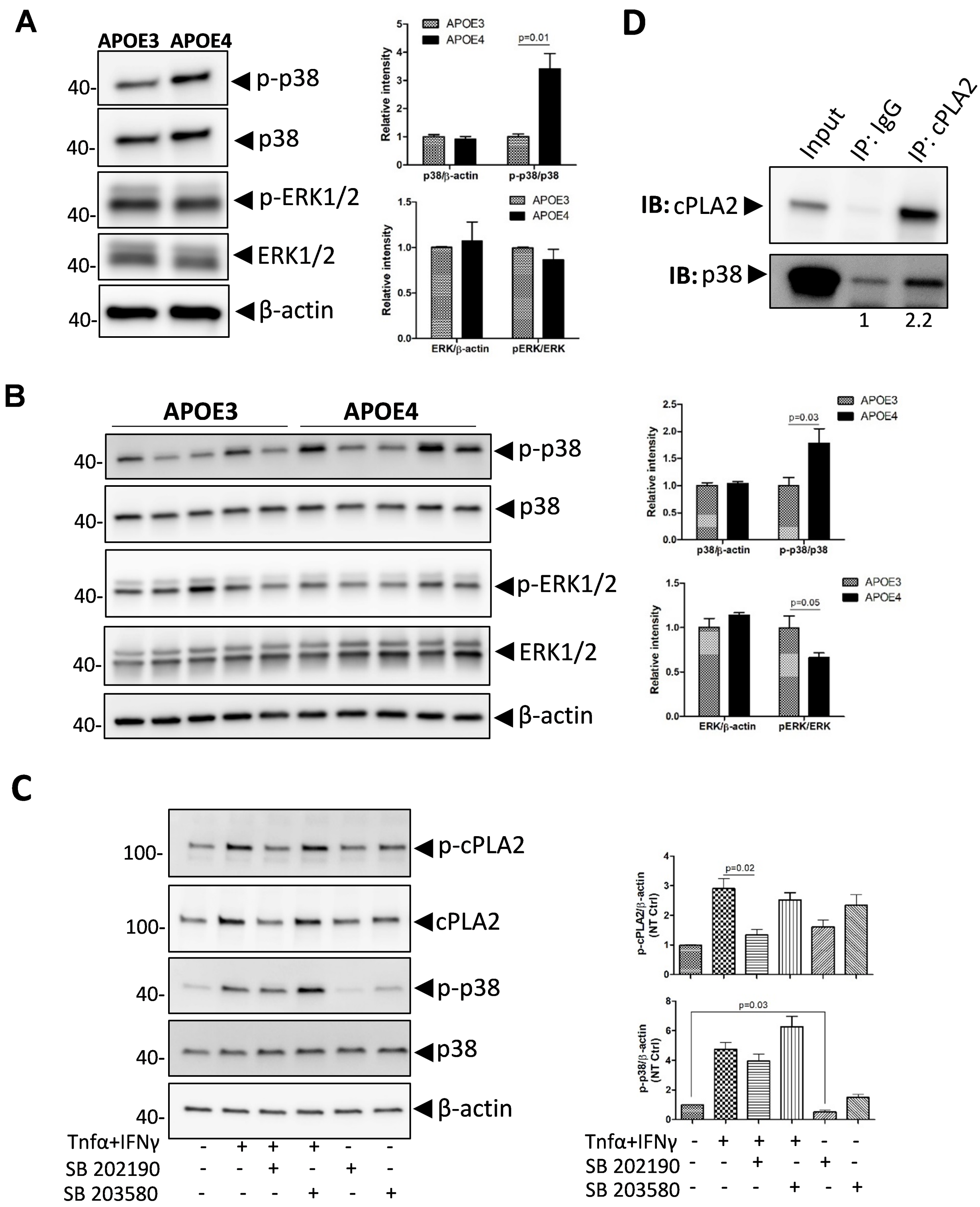

Figure 3

Increased phosphorylated-cPLA2 in APOE4 is mediated by p38 MAPK. A, Phosphorylated and total p38 and ERK levels in primary astrocyte from ApoE3 and ApoE4-TR mice were detected by WB densitometry (left). B, Phosphorylated and total p38 and ERK levels in cortical homogenates from APOE3 and APOE4-TR mice were detected by WB (left). C, ApoE4 primary astrocytes from mouse were pre-treated with p38 inhibitors SB 202190 (10μM) or SB 203580 (10μM) for 20 minutes and then treated with medium or

TNFα plus IFNγ together for 30 minutes. The total and phosphorylated cPLA2 and p38 were detected in the cell lysate by WB (left). D, cPLA2 bound with p38. Immunoprecipitation was performed in the cell lysate of immortalized ApoE4 astrocytes using anti-cPLA2 antibody or species-matched IgG. cPLA2 and p38 were co-detected after immunoprecipitation by WB. WB: Western Blot

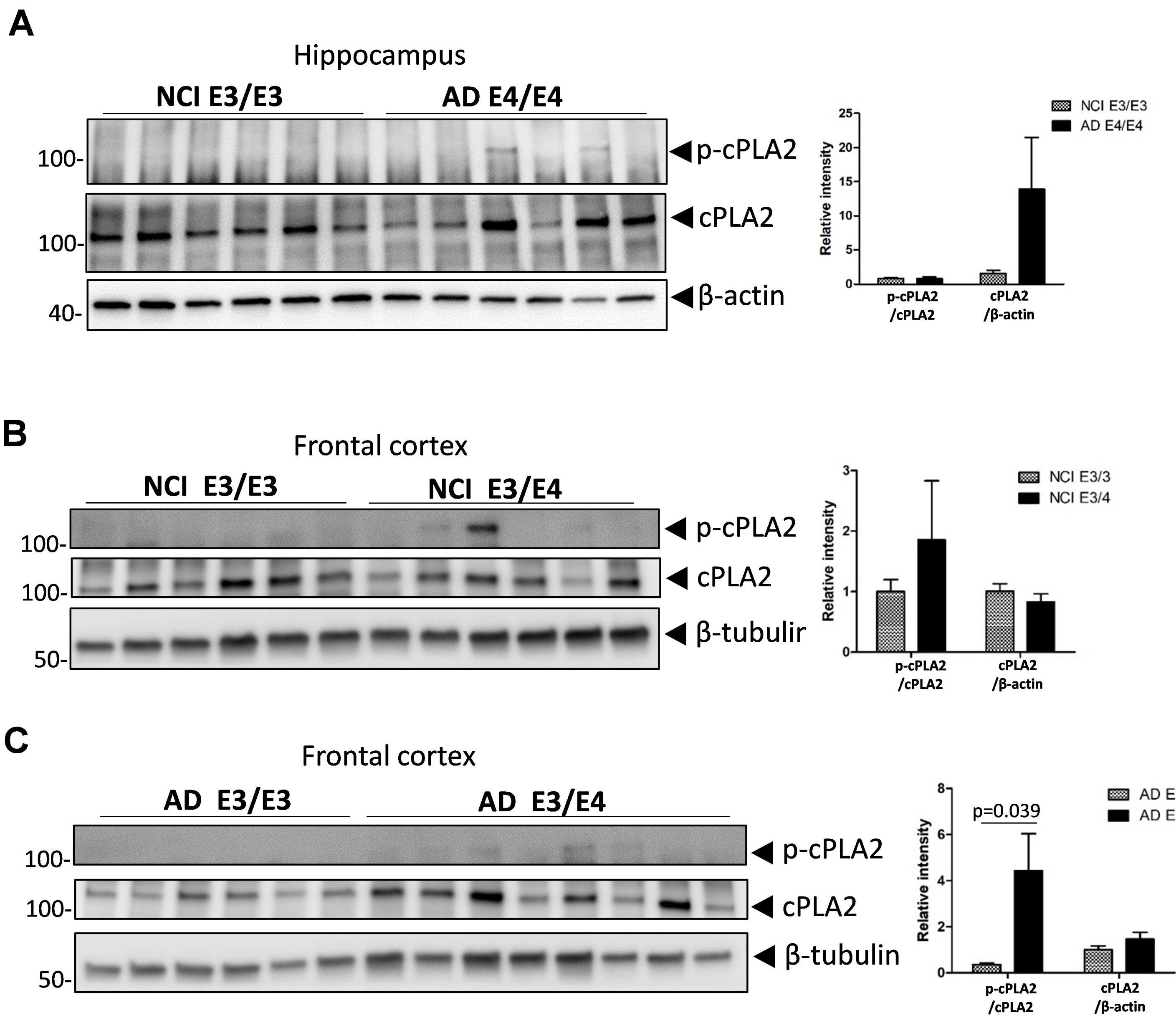

Figure 4

cPLA2 and phosphorylated-cPLA2 levels in the brains of persons with different APOE genotypes. A, p-cPLA2 and cPLA2 protein levels in the hippocampi from persons with no cognitive impairment (NCI) carrying E3/E3 and AD patients carrying E4/E4 were detected by WB (left). Quantification of WB from three independent experiments (right). (n=7 (F5/M2) NCI E3/E3; n=9 (F6/M3), AD E4/E4). B, p-cPLA2, and cPLA2 protein levels in the inferior frontal cortex from persons with NCI were detected by WB densitometry (left). (n=12 (F6/M6), NCI E3/E3; n=10 (F5/M5), NCI E3/E4). C, p-cPLA2, and cPLA2 protein

levels in the inferior frontal cortex from AD patients were detected by WB (left). (n=12 (F5/M7), AD E3/E3; n=10 (F6/M4), AD E3/E4). WB: Western Blot

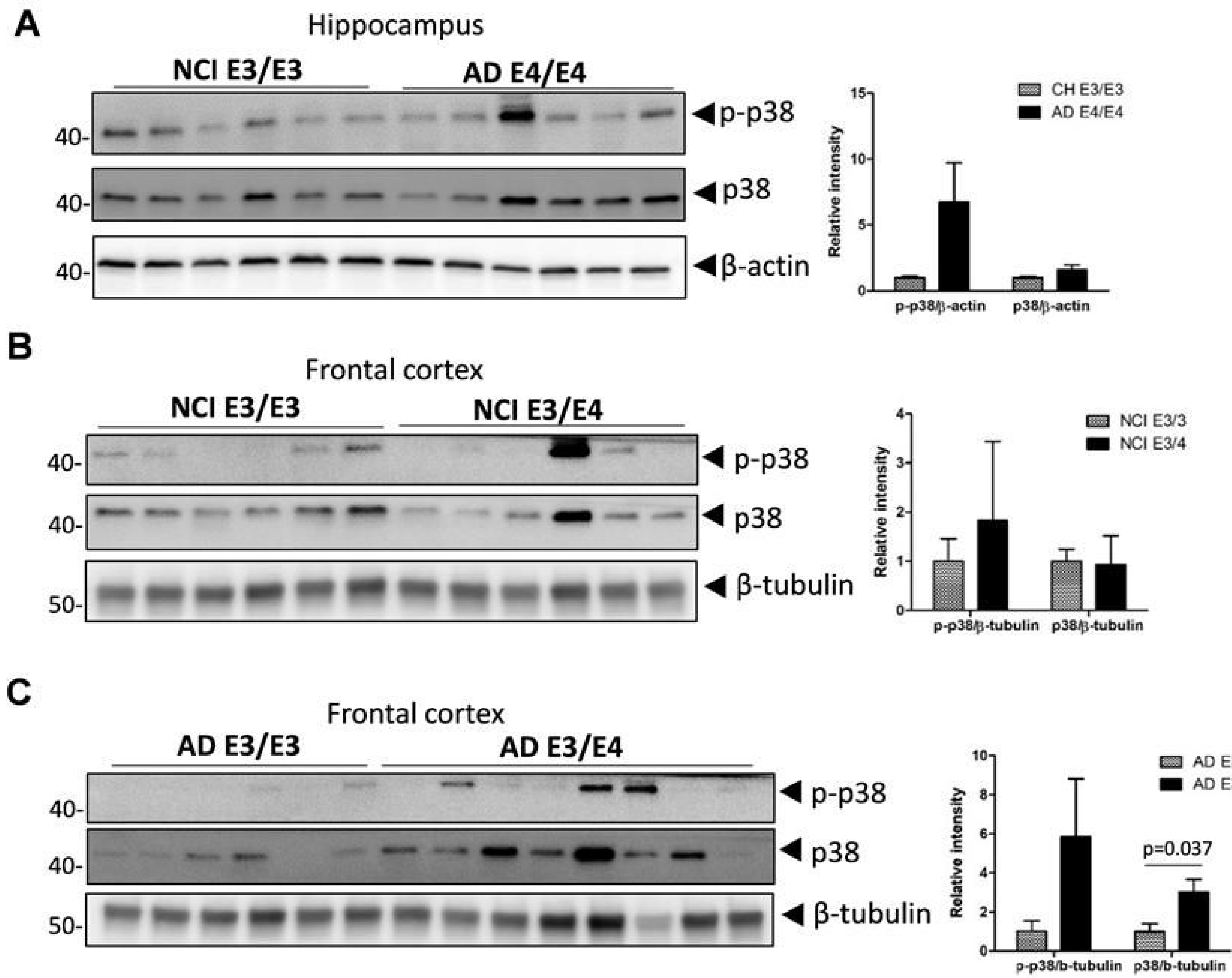

Figure 5

p38 levels in the brains of humans with different APOE genotypes. A, p-p38 and p38 protein levels in hippocampus from persons with no cognitive impairment (NCI) carrying E3/E3 and AD patients carrying E4/E4 were detected by WB (left) ((n=7 (F5/M2) for NCI E3/E3; n=9 (F6/M3) for AD E4/ E4). B, p-p38 and p38 protein levels in inferior frontal cortex from persons with NCI were detected by WB densitometry (left) (n=12 (F6/M6) for NCI E3/E3; n=10 (F5/M5) for NCI E3/E4). C, p-p38 and p38 protein level in inferior frontal cortex from AD patients were detected by WB (left) (n=12 (F5/M7) for AD E3/E3; n=10 (F6/M4) for AD E3/E4). WB: Western blot

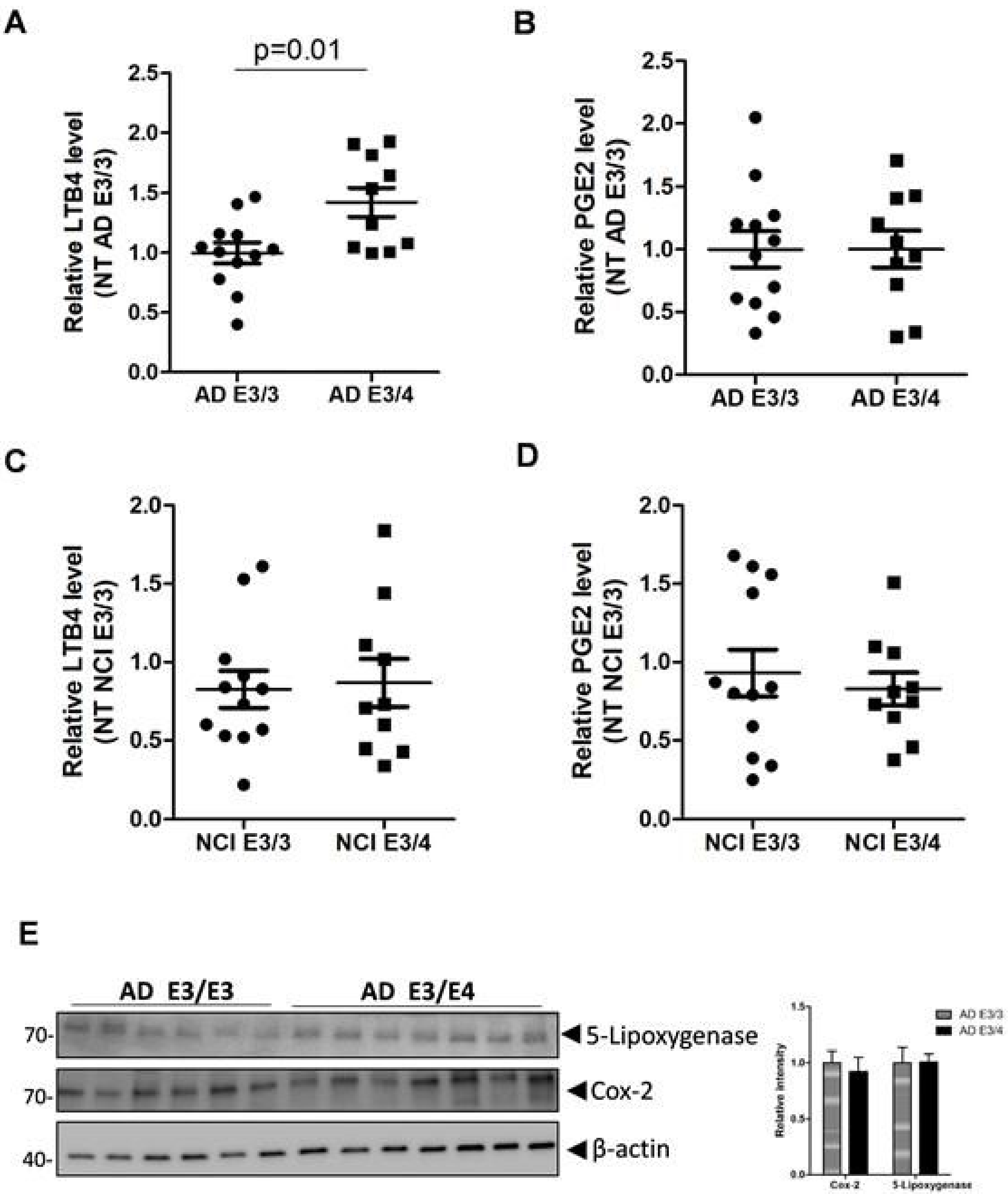

Figure 6

LTB4 and PGE2 levels in the cortex of humans with different APOE genotypes. LTB4 (A, C) and PGE2 (B, D) levels in the inferior frontal cortex of AD patients (A, B) and NCI participants (C, D) with different APOE genotypes. E, 5-Lipoxygenase and cyclooxygenase 2 protein levels in inferior frontal cortex from AD patients were detected by WB (left) (n=12 (F6/M6) for NCI E3/E3; n=10 (F5/M5) for NCI E3/E4; n=12 (F5/M7) for AD E3/E3; n=10 (F6/M4) for AD E3/E4).

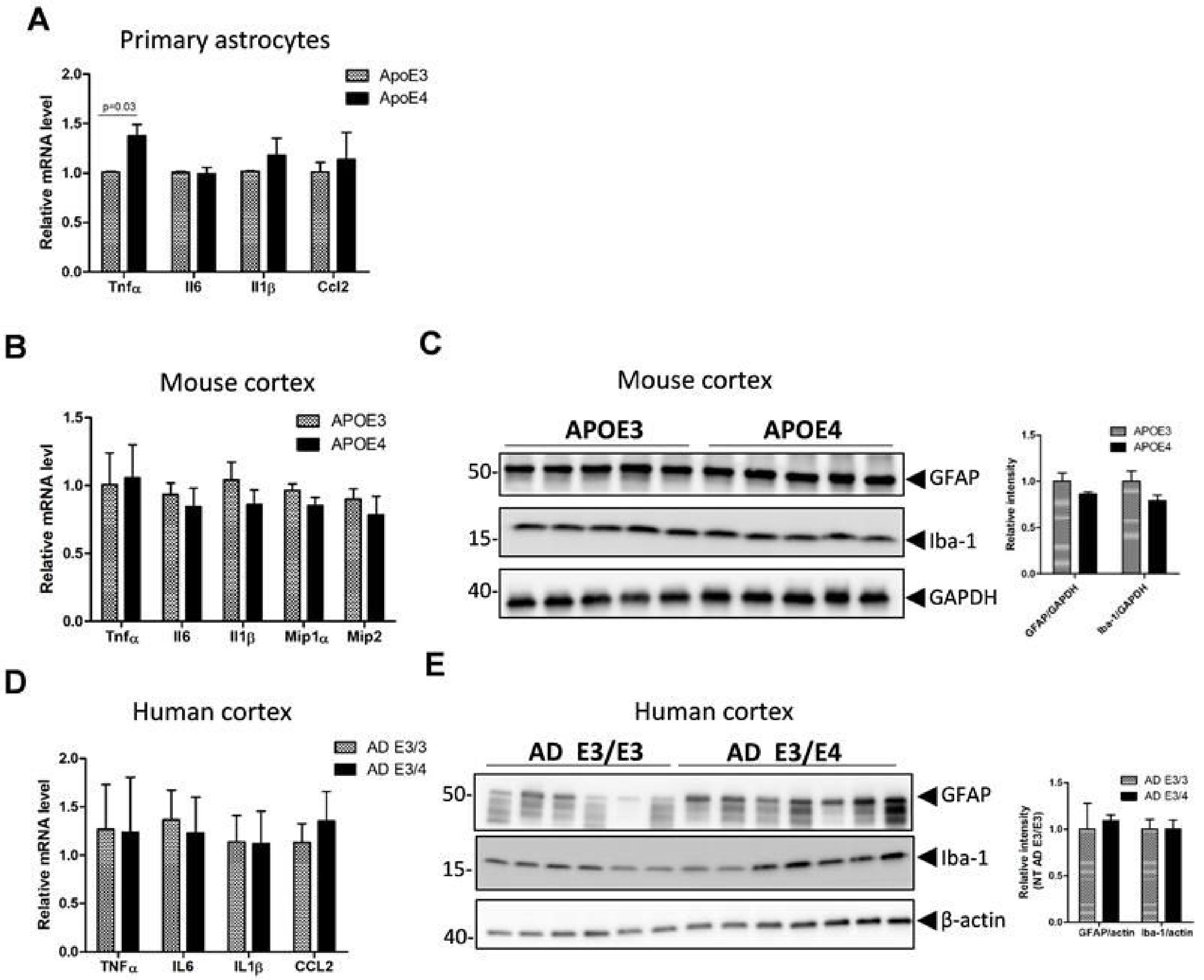

Figure 7

Inflammatory responses in primary astrocytes, mouse, and human cortex with different APOE genotypes. A, mRNA levels of proinflammatory markers in the primary astrocyte from ApoE3-TR or ApoE4-TR mice. B, mRNA levels of proinflammatory cytokines in the cortex of ApoE3-TR or ApoE4-TR mice. C, GFAP, and Iba-1 expression in the cortex of ApoE3-TR or ApoE4-TR mice. (n=5, 3 males and 2 females for B and C). D, mRNA levels of proinflammatory markers in inferior frontal cortex from AD patients. E, GFAP, and Iba-1 expression in inferior frontal cortex AD patients. (n=12 (F5/M7) for AD E3/E3; n=10 (F6/M4) for AD E3/E4).

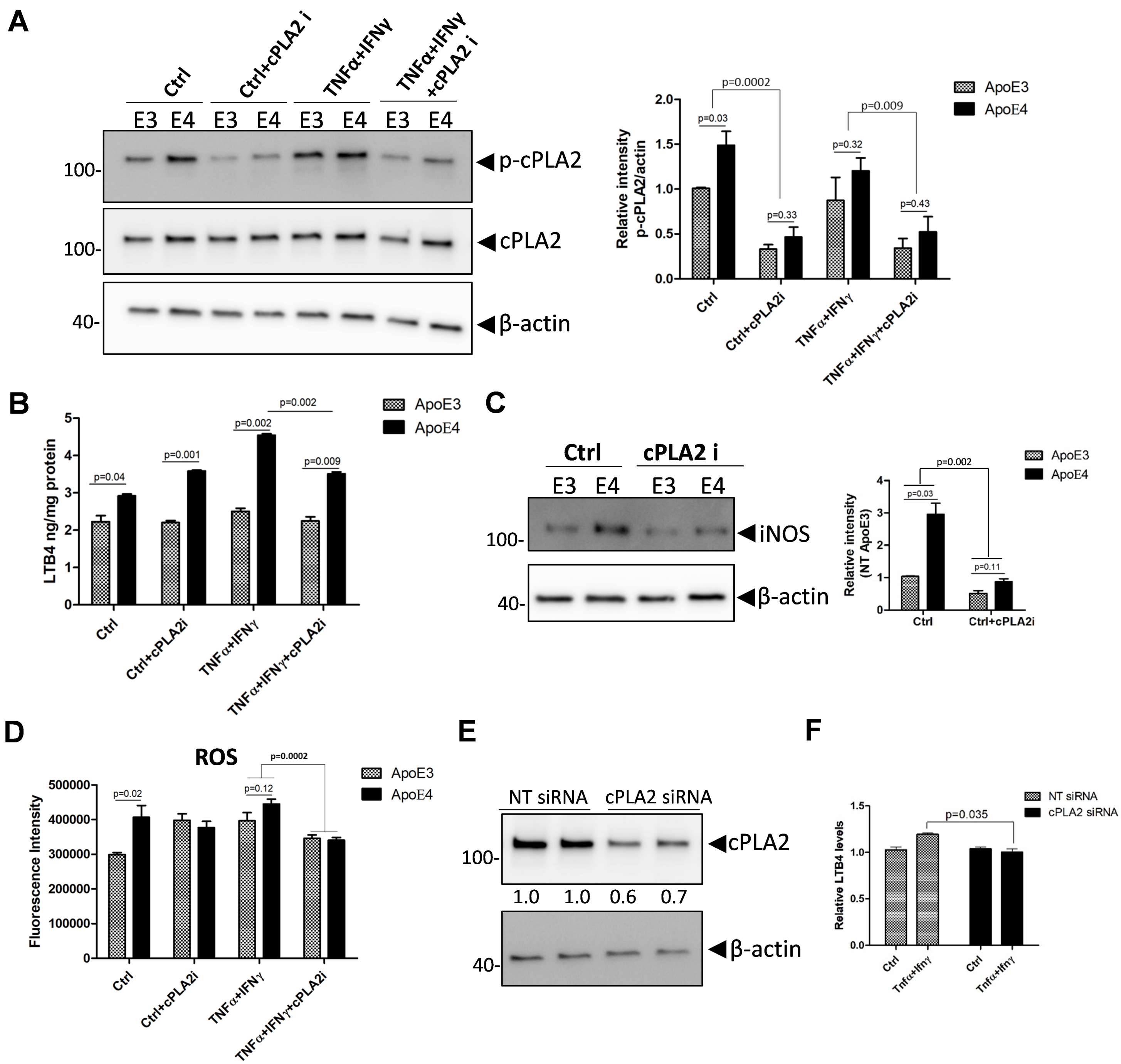

Figure 8

Inhibition of cPLA2 reduces ApoE4 mediated up-regulation of LTB4, ROS, and iNOS levels. (A-C) ApoE3 and ApoE4 primary astrocytes from mice were pre-treated with cPLA2 inhibitor- pyrrophenone (500nM) for 30 min and then treated with medium or TNFα plus IFNγ together for 18 hours. Total and phosphorylated-cPLA2 were detected by WB (left). LTB4 levels in the culture medium were measured by the assay kit (B). iNOS expression was detected by WB (left). Quantification of WB from three independent experiments (right) (C). D, ApoE3, and ApoE4 primary astrocyte were pre-treated with cPLA2 inhibitor-pyrrophenone (1μM) for 30 min and then treated with medium or TNFα plus IFNγ together for

24h. The ROS level were detected by the DCFDA probe. E, F, ApoE4 primary astrocytes were transfected with cPLA2 siRNA (10nM) or Non-target (NT) siRNA (10nM) for 48 hours and then treated with medium or TNFα plus IFNγ together for 24 hours. cPLA2 protein levels in cell lysate were detected by WB (E). LTB4 levels in the culture medium were measured by the assay kit (F). Two-way ANOVA was used in A, C, and D for group comparisons.

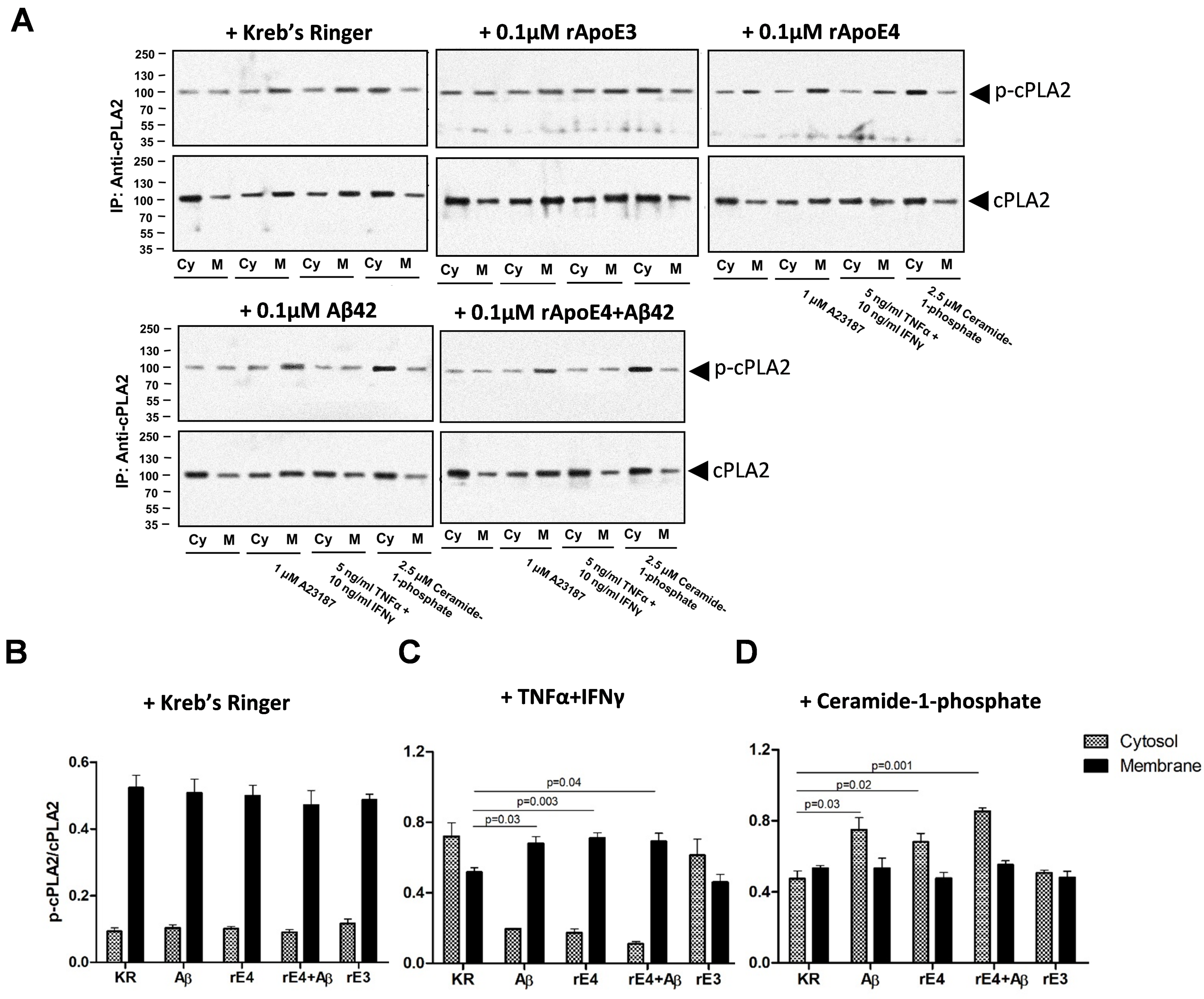

Figure 9

ApoE4 and Aβ42 induced cPLA2 activation in human postmortem frontal cortical synaptosomes. A, Synaptosomes were incubated in oxygenated Kreb's Ringer with different reagents: rApoE3, rApE4, Aβ42, Aβ42/rApoE4 for 30 min, followed by 15 minutes incubation with Kreb's-Ringer (control), TNFα/IFNγ or ceramide-1-phosphate, respectively. The synaptosomes were harvested and homogenized, and the membrane and cytosolic fractions of synaptosomes were isolated by centrifugation. cPLA2 was enriched in both fractions by immunoprecipitation with anti-cPLA2 antibodies, and the phosphorylated and total cPLA2 were detected by WB. B-D, Densitometric quantification of blotting shown in A.

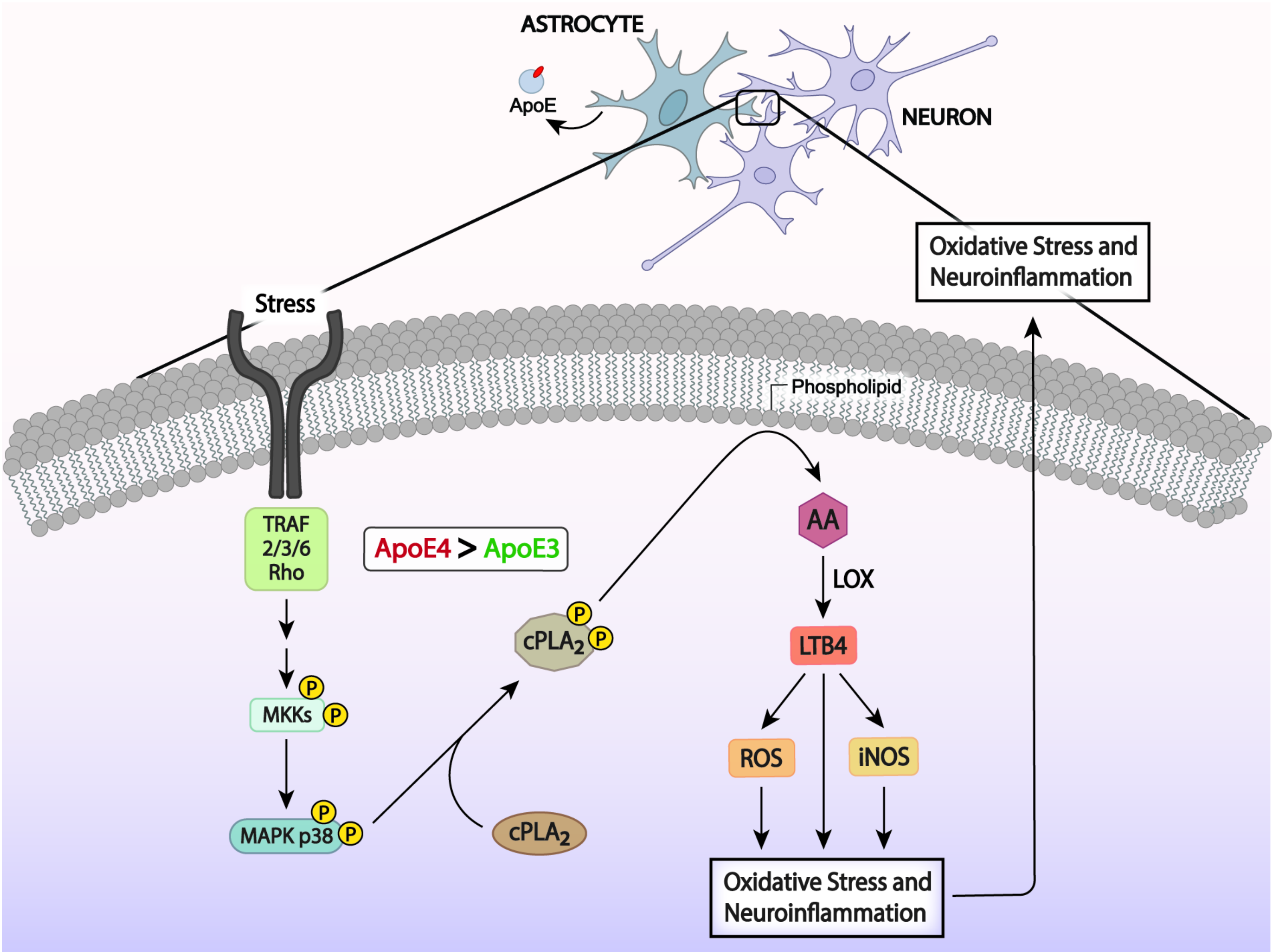

Figure 10

Illustration of ApoE4 in astrocytes inducing greater cPLA2 activation than ApoE3 through the p38 MAPK pathway, leading to more LTB4, iNOS, and ROS production. increased oxidative stress, and neuroinflammation.

Supplementary Files

This is a list of supplementary files associated with this preprint. Click to download.

- FigureS1.tif
- FigureS2.tif
- FigureS3.tif